PREDICTING PACKAGE DEFECTS: QUANTIFICATION OF CRITICAL LEAK SIZE

by

Matthew Joseph Gibney IV

Thesis submitted to the Faculty of Virginia Polytechnic Institute and State University in partial fulfillment of the requirements for the degree of

Master of Science

in

Food Science and Technology

Dr. Joseph E. Marcy, Chair

Dr. Cameron R. Hackney

Dr. Barbara A. Blakistone

Dr. Richey M. Davis

June 30, 2000

Blacksburg, VA

Keywords: threshold leak size, leakers, microbial ingress, package sterility, hermetic seal

PREDICTING PACKAGE DEFECTS:
QUANTIFICATION OF CRITICAL LEAK SIZE

Matthew Joseph Gibney IV

(ABSTRACT)

Threshold leak sizes and leak rates were calculated for a number of liquid food products exhibiting a wide range of surface tension and viscosity values. From this data, one can see that mathematically, under typical pressure differentials generated in food packages (≤ ±34.5 kPa), a leak will never start through a 2 μm defect. The calculated leak rates were compared to calculated evaporation rates. The evaporation rate exceeds the leak rate at lower sized microholes (2, and 5 μm diameter) under typical pressure differentials found in food packages. If the liquid, typically aqueous in food products, is evaporating off faster than the leak itself, then there will be solids left behind that could effectively plug the leak.

The critical leak size is the size micro-defect that allows microbial penetration into the package. The critical leak size of air-filled defects was found to be 7 μm at all pressures tested. This size is considerably important to food packagers because this is when sterility of the package is lost. Previous leak studies have shown that the critical leak size for liquid-filled defects coincide with the threshold leak size and pressure. If this is in fact true, then air-filled defects should exhibit a larger critical leak size than the liquid-filled defects. In this study, air-filled defects were examined. A bioaerosol exposure chamber was used to test micro-defects, nickel microtubes of known diameters 2, 5, 7, 10, 20, and 50 μm hydraulic diameters, against pressure differentials of 0, -6.9, -13.8, and -34.5 kPa.

Acknowledgements

I would like to acknowledge my graduate committee members, Dr. Barbara Blakistone, Dr. Richey Davis, and Dr. Cameron Hackney for being very insightful during the entire research project. A special thanks goes to my graduate committee chairman Dr. Joe Marcy for his advice and general wisdom. I would like to thank the Center for Aseptic Packaging and Processing Studies (CAPPS) and the National Food Processors Association (NFPA) for financial support of this project. I would like to thank Dr. Scott Keller for all of his help, Harriet Williams, John Chandler, and Brian Smith for their help with equipment. Thanks to Dr. George Lacy for the bacteria and to Dr. Hans Carter for his expertise in biostatistics.

Thanks to the good folks in my office, Eric Suloff, Dan Martin, and Kali Phelps for advice on homework and the thesis. Thanks to my good friends Valerie Green, Omid Yamini, Paul Swanson, and Kristian Thor for the good times. Thanks to Selester Bennett for both intellectual and not-so-intellectual conversation while puffing Excaliber stogies. Thanks to my partners in music Cole Bolling, Jason Laughlin, and the wonderful voice of Karen Creighton.

TABLE OF CONTENTS

LIST OF TABLES AND FIGURES

TABLES

FIGURES:

INTRODUCTION

The need for one hundred percent on-line package leak detection is a top priority for aseptic food processors (Keller, 1998). Package integrity is vital to both food quality assurance and food safety (Stauffer, 1990). There are many package inspection systems available that rely on physical testing of the package to indicate the possibility of microbial contamination. A physical test is much quicker and more sensitive than a microbial challenge test, however, a microbial challenge indicates conditions for microbial contamination. Critical limits for microbial contamination have not yet been examined thoroughly enough to compare physical tests to microbial tests. In 1988, Virginia Chamberlain, then a sterility expert in the compliance division of FDA's Center for Devices and Radiological Health, said, "If something fails a certain physical test, what does that mean in terms of compromising the product's sterility? If a package contains a pinhole, how big does that pinhole have to be?" (Bryant, 1988).

An aseptic food package is defined as a hermetically sealed container that holds sterile food and maintains the integrity of the food throughout a long shelf life (Yeh and Benatar, 1997). According to Clifford M. Coles, aseptic processors must ensure three things: "that the product remains shelf stable, that it does not experience any commercial failure, and that it does not represent a public health hazard due to microbial spoilage." (Anonymous, 1998) Sterility maintenance assurance is of paramount importance for the food processor. Food safety is an integral part of any quality assurance standards. From an economic standpoint, the food processor must avoid financial losses associated with foodborne illness and product reworking (Anonymous, 1998; Anderson, 1989).

Food products that support pathogen growth and/or spoilage organism growth must either be sterilized after packing or packaged aseptically. These processes alone, however, are not the only assurance of sterile contents. If the package is defective to a point to allow infiltration of pathogens or spoilage organisms, then the package is no longer sterile. The package could be inadequately sealed, or the package material itself

may contain leaks of sufficient size to allow ingress of microorganisms. A leak, as defined by the American Society for Testing and Materials, is "a hole, or void in the wall of an enclosure, capable of passing liquid or gas from one side of the wall to the other under action of pressure or concentration differential existing across the wall, independent of the quantity of fluid flowing" (ASTM, 2000). A leak large enough to allow microbial contamination has been referred to as the critical leak size.

Leakers in cans are typically caused post processing. Defects that cause post process leakage in metal cans include microleaks, defective seams, abrasions, and corrosion (Stersky et al., 1980). A microleak could be considered a hole with a diameter that falls below the threshold of human visual inspection. Microleaks can either occur temporarily or remain a permanent defect (Gilchrist et al., 1989). These leakers are only now beginning to be studied in terms of critical leak size.

One of the main factors that directly affects the critical leak size is whether or not the microleak is filled with liquid. Early leak studies with contaminated cans showed that microorganisms penetrated the can through a liquid filled defect (Amini et al., 1979; Davidson and Pflug, 1981; Guazzo, 1994; McEldowney et al., 1988; Put et al., 1972; Put et al., 1980; Stersky et al., 1980). The microorganisms were thought to traverse the defect either by motility or pressure differentials found within the liquid filled defect itself (Amini et al., 1979; Hurme et al., 1997; Kamei et al., 1991; Keller, 1998; McEldowney et al., 1988; Pflug et al., 1981; Placencia et al., 1986;). A liquid filled microleak effectively links the interior contents to the external environment. It is debatable as to whether or not an air-filled defect will pose the same risk for microbial contamination as a liquid-filled defect.

Since a microleak that is liquid filled should more readily allow the passage of microorganisms to the interior of the package, it is crucial to critical leak size studies to understand the mechanics behind how a microleak becomes liquid filled. It is also necessary to test defects that are filled with air and compare the liquid and air-filled defect's critical leak size. Thus solidifying the assumption that a critical leak size is indeed smaller for liquid-filled defects than it is for air-filled defects.

Previous research has linked the critical leak size of a micro-defect to the size micro-defect that allows initiation of leakage at a particular pressure (Keller, 1998). An equation was developed that shows that the initiation of a leak is dependent on the surface tension of the liquid food product as well as the micro-defect size (Keller, 1998).

The first objective of this research was to quantify threshold leak pressures and leak rates for liquid food products with a wide range of surface tensions, viscosities, densities, and package size. This will allow the threshold leak size to be calculated for typical internally generated pressures in the package.

The second objective of this research was to biotest air filled defects with a bioaerosol exposure chamber to compare threshold leak size and critical leak size. Since the critical leak size has been linked to the threshold leak size by bioaerosol testing liquid-filled defects and comparing them to the threshold leak size (Keller, 1998), it is necessary to test whether an air-filled defect will have a different critical leak size.

SECTION I

LITERATURE REVIEW

Flexible and Semi-Rigid Packages

Flexible and semi-rigid packages were developed as an alternative to cans. They are generally constructed of layers of polymer, foil, and/or paperboard. Different combinations of these materials yield different strength and flexibility profiles.

Flexible package applications have increased dramatically in the food and medical industry. Packaging experts estimate that 50 to 70% of all recalls of medical devices are due to packaging defects (Bryant, 1988). Early suggestions for the packaging leakers included wrinkles in the seal area, or holes in the packaging material itself (Lampi, 1980). It has also been rationalized that a defect can either occur temporarily or remain a permanent defect. This is very common in flexible packages, in which an intentionally formed pinhole can reduce in size due to the flexibility of the package (Gilchrist et al., 1989).

Typically, in a flexible package, the seal area is coated with a heat sealable coating. These films can be bonded together by the application of heat. The seal area is where most leaks would be expected to occur. Leak studies done on the quality of peanuts indicated that the rancidity was cause by increased oxygen levels entering the package through leaks in the seal (Goode and Soutar, 1995). A wrinkle in the seal area may form a channel leaker because the leaker length is significantly larger than the diameter.

Leakage Studies of Flexible Packaging

Post-process contamination of cans and retort pouches is a major concern for food safety and spoilage (Put et al., 1972). A study in 1983 showed that bacteria typically contaminating the recycled cooling water of a still retort are of the *Clostridium* species (Thompson, 1983). The early studies provided some guidelines on how to properly handle packages after processing to avoid post-process contamination.

The correlation between post-process contamination with handling and storage conditions was proved by testing the effect of post-process handling procedures on wet and dry containers (Michels and Schram, 1979). Using holes punched with a needle of 100 μm diameter, it was shown that the incidence of post-process contamination was 90% if the package was manually removed from the retort and stored wet. The occurrence of post-process contamination dropped sharply to 10% if the container was removed manually while wet, then dried before storage. The contamination rate decreased to less than 1% if the packages were cooled in chlorinated water and dried before removal and storage (Michels and Schram, 1979).

Most of the early sterility assurance tests used the immersion biotest, in which a package filled with food or bacterial media is submerged in a bath of bacteria. After a given amount of time, the interior of the package is tested for bacterial penetration. The concentration of bacteria used in an immersion biotest also dictates the probability of microbial ingress (Anema and Schram, 1980; Blakistone et al., 1996). Using 100 μm diameter holes, it was shown that the percentage of contaminated packages decreases when the bacterial concentration decreases (Anema and Schram, 1980).

The pressure differential between the inside and outside of the container was considered to be another factor involved in microbial infiltration. Early studies showed that a can with a headspace vacuum of 400 mm Hg is more prone to microbial contamination than one that is equilibrated to the atmosphere (Put et al., 1972). A study in 1988 also showed this situation, as the number of bacteria passing through a filter with a pore size of 5 μm increased as a vacuum was applied (Bankes and Stringer, 1988). This study was also confirmed in a later study using a variety of pore sizes for the filter system (McEldowney and Fletcher, 1990a). The higher the viscosity of the liquid in the container being tested the lower the bacterial contamination rate. This is because the actual flow rate is so slow that the highly viscous liquid could not reach the outside of the package, thus it did not form a complete liquid channel (McEldowney and Fletcher, 1990b).

Early attempts at linking physical leak detection tests to microbial biotests in flexible packages have failed to produce reproducible results. These failures can be

attributed to the deformity of flexible package material. When a micro-sized defect is intentionally manufactured in this material, the flexibility of the package can either increase or decrease the microhole size that was originally produced. This was the case when an immersion biotest was compared to a fluorescent dye test and a helium test (Gilchrist et al., 1989). The initial microhole sizes of the package ranged from 17 to 175 μm either formed by using a laser or a metal rod to drill through flexible retort pouches. The fluorescent dye and helium tests both indicated leakage far more reliably than the immersion biotest. Taken at face value, the critical leak size looked like it was 20 μm, even though negatives for microbial ingress appeared at larger defect sizes. The question as to why the microbial test did not match the physical tests was answered when the defects were measured after the test. The initial hole sizes had all decreased by varying degrees (Gilchrist et al., 1989). So when did the bacteria actually leak into the package? It could have been at any size during the test knowing that the material is flexible.

The critical leak size for optimal microbial penetration could only be found using a straight defect that does not change significantly in shape or size during a biotest. To address this problem, an immersion biotest was done using semi-rigid aseptic cup lids and retort trays with laser-drilled holes of diameters ranging from 10 - 20 μm. Microbial ingress was found down to the 10 μm hole, so there cannot be a quantitative statement as to what the critical leak size actually is (Hurme et al., 1997).

A package will never encounter such harsh conditions that are typically used in immersion biotesting where the concentration of bacteria can approach 10^9 CFU/ml (Guazzo, 1994). A newer test method that more closely represents conditions that a package might experience is the spray cabinet - bioaerosol exposure method (Reich, 1985; Placencia et al., 1986; Chen et al., 1991; Guazzo, 1994; Keller et al., 1995, 1996, 1998).

In 1991, an immersion biotest was compared to a spray cabinet biotest (Chen et al., 1991). The pinhole orifices were 5, 10, and 15 μm in diameter and made of a nickel alloy with a specific pinhole through the middle. The spray cabinet results indicated leakage at all micro-orifice sizes, however, the immersion method proved to be less sensitive than the spray cabinet method (Chen et al., 1991). These results could be

attributed to the threshold leak pressure not being surpassed for each micro-orifice size in the immersion test. The spray cabinet, however, was believed to generate a pressure on the outside of the micro-orifices, thus aiding in microbial penetration (Chen et al., 1991).

The critical leak size was suggested to fall below 10 μm from examining results from an immersion biotest done using nickel microtubes of 10 and 20 μm of lengths 5 and 10 mm sealed into plastic pouches tested against bacterial concentrations of 10^2 CFU/ml and 10^6 CFU/ml (Blakistone et al., 1996). The test concentration of 10^6 CFU/ml was found to be significant for microbial ingress of motile organisms. The same concentration was found to be significant using a bioaerosol exposure chamber testing the same pouches with the same nickel microtube sizes (Keller et al., 1996).

The bioaerosol exposure method was also employed to study the critical leak size of liquid-filled defects using nickel microtubes with known, unchanging diameters down to 2 μm (Keller, 1998). The critical leak size was found to be the same as the threshold leak size at the threshold leak pressure (Keller, 1998). There were also experiments to determine the effect of motility and size of bacteria on the critical leak size. Three different bacteria, *Pseudomonas fragi* Lacy-1052, *Bacillus atrophaeus*, and *Enterobacter aerogenes*, were used. There were no significant differences found between the species used and the critical leak size (Keller, 1998).

LEAKAGE

A leaker is a package that has a hole of sufficient size to allow passage of fluid from the inside of the package across the wall of the package. The driving force of leakage of liquids and gases is the pressure differential across the leak (Morton, 1987; Guazzo, 1994).

Leakage is described in units of volume passing through the leak per unit time. Typically, the units of measure used to indicate leakage rates are standard cubic centimeters per second (std cm^3/s). A std cm^3/s means that the leak rate is for a quantity of fluid at 1 atmosphere (101.3 kPa, 14.7 psi) and 20°C. Gas leakage requires the pressure to be specified because gas is a compressible fluid. An increase in pressure of a

gas results in a significant volume change. Another common unit for gas leakage is Pascal cubic meters per second ($Pa \cdot m^3/s$). Since liquid is an incompressible fluid, the pressure term is not required and the leakage rate can be simply specified by volume over time. The conversion factor of $Pa \cdot m^3/s$ to cm^3/s is 9.87. The research presented here uses cm^3/s, which is exactly equal to ml/s.

Leak Rate Specification

There are three different flow patterns associated with leakage. The most rapid leakage is characterized by turbulent flow, followed by laminar flow, and the slowest leak rate called molecular flow. Each of these different flow patterns is characterized by different flow rates and shown below using gas flow rate units ($Pa \cdot m^3/s$). Turbulent flow rates are typically greater than 10^{-3} $Pa \cdot m^3/s$ (Anonymous, 1982; Morton, 1987). The leakage rate for laminar flow is between 10^{-2} $Pa \cdot m^3/s$ and 10^{-7} $Pa \cdot m^3/s$ (Amini et al., 1979; Anonymous, 1982; Eisenberg, 1979; Loeb, 1961; Morton, 1987). The equations used for laminar flow rates are also applicable to the movement of liquid through capillaries. Molecular flow is below 10^{-6} $Pa \cdot m^3/s$ (Anonymous, 1982; Morton, 1987). This type leakage is so slow that it only describes the leakage of gases (Guazzo, 1994). For the microleaks that are considered in this paper (< 50 μm), the flow is laminar. Turbulent flow is too fast and molecular flow is too slow.

A package is considered leak free when the leak rate is occurring below an established leak rate specification. It has been argued that if a leak is so small that no liquid can pass through, then no microorganisms will be able to pass through either (Morton, 1989). With this frame of thinking, the lowest leak rate that could allow microbial penetration into a package would be close to 10^{-5} $Pa \cdot m^3/s$ (Anonymous, 1982).

Threshold Leak Size

Since a microleak that is liquid filled should more readily allow the passage of microorganisms to the interior of the package (Amini et al., 1979; Hurme et al., 1997; Kamei et al., 1991; McEldowney et al., 1988; Pflug et al., 1981; Placencia et al., 1986; Keller, 1998), it is crucial to critical leak size studies to understand the mechanics behind

how a microleak becomes liquid filled (Keller, 1998). By mathematically modeling leak situations, threshold leak sizes and threshold leak pressures can be theoretically described for various packages and liquid food products. The threshold leak size is considered the smallest size microhole that allows a liquid to leak from a package (Keller, 1998). This term is different from the critical leak size although the critical leak size is generally the same size as the threshold leak size. The threshold leak pressure is the pressure required to initiate liquid flow into the microhole (Keller, 1998).

Once the leak is initiated, the liquid must flow through the defect at a rate that exceeds the rate of evaporation of the liquid (Davis, 1999; Keller, 1998). This is quite important with microleaks because the leakage rate is usually so slow that the liquid will evaporate leaving solids behind that effectively block the flow, thus resealing the leak.

The direction of the flow is also very important. The pressure differential from the inside of the package to the outside determines the flow rate and more importantly, the direction of flow. Food packages can have positive pressure or negative pressure (vacuum) inside the package. If the sum pressure on the inside of the package is greater than the sum pressure on the outside of the package, then flow will be from the inside to the outside (positive flow). If the sum pressure on the inside is less than the sum pressure on the outside than the flow will be in the opposite direction (negative flow). This "negative" flow is important in retort cooling water operations where the package is cooled in a bath of water. The cooling water creates a vacuum on the inside of the package as heat is lost and the gas on the inside of the package compresses. This results in the ingress of cooling water into the package if a leak is present. If the cooling water is contaminated with microorganisms, then the package sterility is jeopardized (Michels and Schram, 1979; Put et al., 1972).

To quantify the initiation of flow, the flow rate (including the direction of flow), and the evaporation rate of various liquid food products leaking from different packages, a basic understanding of fluid flow mechanics is needed.

FLUID FLOW

A fluid can be defined as a material that continuously deforms under the application of shear stress. The rate of deformation is proportional to the shear stress, which means that it flows. When the stress is removed, the fluid does not retain nor attempt to retain its original shape.

When a force acts perpendicular to a surface, it is termed normal stress, or pressure. When a force acts parallel to the surface, the stress is considered shear stress. The reaction of materials to shear stress lends to the broad categorization of materials as plastic, elastic and fluid.

When shear stress is applied to a plastic material, it deforms continuously, the rate of deformation being proportional to the shear stress, thus it flows. However, when the stress is removed, the material partially recovers to its original shape. An elastic solid, on the other hand, undergoes finite deformation, in other words, it does not flow. Upon removal of the stress, the elastic solid returns to its original shape.

Both liquids and gases are considered fluid. Liquids are called incompressible fluids because when normal stress (pressure) is applied to it there is no appreciable volume change. A gas is called a compressible fluid because an increase in pressure results in a significant volume change.

Physical Properties of a Fluid

The macroscopic properties of a fluid reflect its underlying molecular structure. There are some physical properties that are very significant in indicating how a fluid reacts to applied forces. The forces that are of prime interest in fluid mechanics are the density, viscosity and surface tension. Other properties are not as closely coupled to fluid motion.

Density

The density of a fluid is defined as the ratio of the fluid's mass to its volume. The symbol ρ typically represents the property of density. It is usually expressed in kg/m^3. The density of a fluid determines the acceleration of a volume of fluid. Fluids of low density, gases, accelerate more readily than high-density fluids, liquids, when the same force is applied to the same volume. This is why it is more difficult to wade through water than it is to walk through air.

The density of a fluid is a function of its temperature and pressure. If pressure is held constant and the temperature is increased, then the density decreases because a fixed mass of fluid expands with the increasing temperature. The opposite of this also holds true. If the temperature is held constant and the pressure is increased, then the density increases.

A hydrometer can be used to measure the specific gravity of a liquid. The specific gravity is simply a ratio of the density, ρ, of a liquid to the density of water at 4ºC, ρ_{ref}. The density of water at this temperature is at its maximum and heating above or cooling below this temperature causes the water to expand. If a hydrometer is used for density measurements, then the specific gravity can be multiplied by the ρ_{ref} to obtain the density of the fluid.

Viscosity

Viscosity, μ, is the resistance of the internal layers of fluid to flow. One method of understanding viscosity is through a basic experiment. A fluid filling a space h between two parallel plates is subject to a simple shearing motion. The upper plate moves with a speed **V** while the lower plate remains stationary. If the force, γ, required to move a plate at a speed, **V**, is measured, then it is seen that γ is proportional to **V** and inversely proportional to h for any given fluid. However, there is a proportionality constant that is different for each fluid tested. This proportionality constant is referred to as the viscosity, μ.

If the fluid in between the two plates can be visualized as a stack of thin layers, any thin layer of thickness Δh, must also experience the same stress γ and a corresponding velocity difference ΔV such that:

$$\gamma = \mu \frac{\Delta V}{\Delta h} \qquad \{1\}$$

When γ is the same at all points within the fluid, the velocity difference varies linearly with the distance of the layer to the plate surface. A fluid that exhibits this kind of behavior is known as a **Newtonian** fluid. Most liquids are Newtonian, and all liquids used in this research are of this kind. There are non-Newtonian liquids, but it is much more difficult to describe the stress in these kinds of fluids.

The viscosity of a fluid varies significantly with temperature but very little with regards to pressure. Liquid viscosities decrease with increasing temperature, whereas gas viscosities increase with temperature.

Surface Tension

Both viscosity and density apply to the interior of a fluid that is surrounded by fluid elements. When a fluid element is found at the border of the fluid, though, it is in contact with a dissimilar fluid or solid. The molecules on the interior of the fluid are completely surrounded by the same type molecules, whereas at the interface the fluid molecules are only surrounded by like molecules on one side. The configurational energy of the surface molecules differs from the molecules on the inside. This causes the surface molecules to exist in a state of tension, resisting deformation (Whitaker, 1992).

The surface tension was proven to be the critical food product parameter in determining the threshold leak size and pressure (Keller, 1998). This is because the force acting on the liquid must be strong enough to overcome the surface tension to initiate the liquid flow into the defect.

LEAKAGE EQUATIONS

Threshold Leak Equation

To predict the threshold leak pressures of various package defects, a mathematical model was developed by Keller, 1998. This equation predicts the (imposed) pressure, $\mathbf{P_o}$ (in kPa), required to initiate a leak of a liquid of surface tension, σ (in mN/m), through a microhole of (hydraulic) diameter, $\mathbf{D_h}$ (in μm). The term $\rho\mathbf{gL}$ represents the liquid static head (in kPa), which is the density of the liquid, ρ (in kg/m^3), times the acceleration of gravity, **g** (9.8 m/s^2 on Earth), and the height, **L** (in m), of liquid above the defect in the container. The atmospheric pressure ($\mathbf{P_{atm}}$) is the pressure of the environment surrounding the package, which is 101.3 kPa (14.7 psi) at sea level. The atmospheric pressure term is subtracted from both sides of the equation so that it does not factor into the imposed pressure required to initiate a leak.

The 0.390 is a unitless correction factor. This correction factor was changed from 0.272 to 0.390 due to an incorrect conversion factor in the original equation (Keller, 1998). The correction factor was used to correct the mathematical values to the experimental values obtained for the threshold leak pressure of deionized water and tryptic soy broth (Keller, 1998). It was thought that the correction factor was necessary due to the hydrophilic nature of the nickel microtubes (Keller, 1998).

$$P_o > P_{atm} + \left[\left(\frac{4\sigma}{D_h} - \rho gL\right) \times 0.390\right] \qquad \{2\}$$

The hydraulic diameter allows for the calculation of the diameter of holes with either circular or elliptical shapes. The equation for hydraulic diameter relates the radius **a**, in the X direction, and the radius **b**, in the Y direction.

$$D_h = \frac{2ab}{\sqrt{\frac{a^2 + b^2}{2}}} \qquad \{3\}$$

Hagen-Poiselle Volumetric Flow Rate Equation

The equation used to obtain threshold leak pressure is derived from the famous Hagen-Poiselle equation of volumetric rate of flow. This equation shows the relationship between the volumetric rate of flow of a laminar liquid and the forces that cause the flow. The equation is:

$$Q = \frac{\pi(P_o - P_L)R^4}{8\mu l} \qquad \{4\}$$

where **Q** is the volumetric rate of flow in units of volume per units of time (cm^3/s). The term **π** is the number 3.14159... The radius, **R** (in cm), of the microhole plays a major part in determining the flow rate. This is quite obvious because the radius term is to the fourth power. This creates large differences in flow rate of microholes that are only micrometers different in radius. The viscosity, **μ** (in Pa·s) and the length of the leak, **l** (in cm), decrease the flow rate as they are increased. The pressure differential that drives the leakage is the term **(P_o-P_L)**. **P_o** (in Pa) is the imposed pressure on the inside of the container while **P_L** (in Pa) is the external pressure acting on the outside of the package.

If a positive pressure is generated on the inside of the package, the flow will occur from the inside to the outside. This is dependent on the amount of pressure, **P_o**, being larger than the combined pressure external to the package, **P_L**. External pressure is the combination of a couple of factors. The atmospheric pressure, **P_{atm}**, plays a large role against leakage. This pressure plus the pressure generated by the relationship (**2σ/r**) between surface tension, **σ** (mN/m), and microhole radius, **r** (m), are the forces that act against the flow of liquid. The liquid static head (**ρgL** in Pa) is subtracted from that pressure sum to give the total external pressure acting on the liquid.

$$P_L = P_{atm} + \left(\frac{2\sigma}{r} - \rho g L\right) \qquad \{5\}$$

The Hagen-Poiselle equation for volumetric flow rate not only determines the flow rate, but also the direction of the flow. This is due to the pressure differential term **(P_o-P_L)**. If the pressure on the inside is greater than the combined pressures on the outside, then the difference will be positive, indicating that the flow is from the inside to the outside of the package. Another possibility is if the external pressures are larger than the internal pressure of the package. The negative pressure differential draws liquid or air surrounding the package into the package. The third alternative is for there to be no flow in either direction. This will occur at the threshold pressure, when (P_o-P_L) = 0.

Evaporation Rate Equations

Evaporation should play a major role in the critical leak size determination for various products. Mathematically, the leak rates tend to be so small that the leak rate sometimes does not even surpass the evaporation rate of water. If this happens, it is believed that soluble solids will remain after all of the liquid has evaporated and will block the flow of liquid through the defect.

Evaporation is expressed as a molar evaporation rate in gram moles per second (gmol/s). In order to compare the flow rate to the evaporation rate, the volumetric flow rate must be converted to molar flow rate. This is easily done by first converting the volumetric flow rate, **Q**, to a mass flow rate, **M**, where ρ is the density of the liquid:

$$M = Q \times \rho \qquad \{6\}$$

The mass flow rate is then converted to the molar flow rate, $W_A^{(m)}$, by simply dividing the mass flow rate by the molecular weight of the liquid.

$$W_A^{(m)} = \frac{M}{mw} \qquad \{7\}$$

The evaporation rate of the leaking liquid is determined by the following equation:

$$W_A^{(m)} = K_{xm}\pi r^2\left[\frac{(X_{Ao} - X_{A\infty})}{(1 - X_{Ao})}\right] \qquad \{8\}$$

Where $\mathbf{W_A^{(m)}}$ is the molar evaporation rate (in gmol/s) from a droplet of radius, **r**, surface. The radius in calculations for this paper is considered to be the same as the microhole. This results in half of a sphere to be exposed to the air for evaporation. The term, $\mathbf{K_{xm}}$ (in gmol/cm^{2}s) is the mass transfer coefficient. $\mathbf{X_{Ao}}$ represents the mole fraction of water in air at the droplet's surface, and the mole fraction of water in ambient air, from relative humidity measurements (typically 60% - 80%), is indicated by $\mathbf{X_{A\infty}}$.

$$K_{xm} = \frac{C_f D_{ABF}}{r} \qquad \{9\}$$

Where $\mathbf{C_f}$ is the moles of gas per cm^3 in film and $\mathbf{D_{ABF}}$ is the binary diffusion coefficient for air-water in film. This diffusion coefficient is used only for water evaporating into air. If a liquid food contains two volatile species, such as ethanol and water, than a much more complex terniary diffusion coefficient is needed (ethanol-water-air). The complexity goes far beyond the scope needed for this research, however, the aqueous evaporation rate can be considered a lower bound because the evaporation rate of the terniary system will be faster (Davis, 2000).

The $\mathbf{C_f}$ is an estimation assuming conditions of room temperature.

$$C_f = \frac{n}{V} = \frac{P}{RT} \qquad \{10\}$$

The estimation of the binary diffusion coefficient $\mathbf{D_{ABF}}$ of water in air is

$$D_{ABF} = a\left[\frac{T}{\sqrt{T_{CA}T_{CB}}}\right]^{b}\left(P_{CA}P_{CB}\right)^{1/3}\left(T_{CA}T_{CB}\right)^{5/12}\left[\frac{1}{M_A}+\frac{1}{M_B}\right]^{1/2} \quad \{11\}$$

Where $\mathbf{a}$ = 3.64 x 10^{-4} and $\mathbf{b}$ = 2.334 for water with a nonpolar gas. $\mathbf{T}$ is the room temperature, $\mathbf{T_{CA}}$ is 132 K for air, $\mathbf{T_{CB}}$ is 647 K for water, $\mathbf{P_{CA}}$ is 36.4 atm for air, $\mathbf{P_{CB}}$ is 217.7 atm for water, $\mathbf{M_A}$ is 28.97 g/mol for air, and $\mathbf{M_B}$ is 18 g/mol for water.

$$X_{Ao} = \frac{P_w}{P_{atm}} \quad \{12\}$$

$$X_{A\infty} = \frac{H_R P_w}{100 \cdot P_{atm}} \quad \{13\}$$

Where $\mathbf{P_w}$ is the vapor pressure of water, $\mathbf{P_{atm}}$ is the atmospheric pressure, and $\mathbf{H_R}$ is the relative humidity percent (Davis, 1999).

Most liquid food products are not pure water. There are usually soluble solids or particulate matter in the mixture. Any particulate matter that is larger than the microhole may actually plug the hole. This is merely a probability problem. Soluble solids, on the other hand, may plug the hole after the water has evaporated leaving a plug behind in the hole. This raises the question as to the evaporation rate of a liquid containing these soluble solids. This can be calculated by substituting the vapor pressure of the liquid in question with the vapor pressure of water in equations 12 and 13. These vapor pressures can be found by measuring the water activity, A_w, which is a ratio of the vapor pressure of a food product (P) to the vapor pressure of pure water (P_o) at the same temperature.

$$A_w = \frac{P}{P_o} \quad \{14\}$$

LEAK DETECTION METHODS

Nondestructive leak testing equipment relies on physical testing methods because of their fast test speed, reliability, and repeatability. Most of the current on-line leak testing equipment is based on a variation of the pressure decay test (Kelsey, 1990). A package is enclosed in an air tight chamber, the air around the package is evacuated, and a pressure-transducer system measures any change in the package internal pressure. Ultrasonic leak detection equipment is becoming very favorable to food packagers because it can detect leaks at least as small as 1 μm and operates at the speed of sound (Kelsey, 1990; Jarrosson, 1992). There are other laboratory physical tests that are even more sensitive such as the tracer gas leak and helium leak test (Guazzo, 1994; Morton, 1987; Gilchrist et al., 1985). Dye penetration tests, chemical tracer tests and bubble tests are the most popular destructive leak tests performed in the laboratory (Guazzo, 1994; Hackett, 1996; Morton, 1987; Gilchrist, 1989).

Visual Inspection

This is by far the least sensitive method of leak detection. A human leak inspector looks for leaks on the package. The obvious limitation of visual leak inspection is the human ocular resolution, which has been indicated at 50 μm (Morris, 1999; Harper et al., 1995). Human visual inspection also is prone to operator skill variability, fatigue and error (Morris, 1999). Generally speaking, human visual leak inspection has a sensitivity of 10^{-2} Pa·m^3/s (Morton, 1987; Guazzo, 1994). There is simply not enough sensitivity with this inspection method to be solely relied on in an industrial food packaging line.

Bubble Testing

The bubble test is a quick and inexpensive way to determine if a leak is present. The bubble test gives a rough estimate of the leak rate by immersing the container in a water bath that may or may not contain detergent to aid in bubble formation and then counting the number of bubbles that emanate from a hole during a certain period of time.

The number of bubbles can be approximated to a volume and then divided by the time in seconds. The sensitivity of this test ranges between 10^{-2} Pa·m^3/s and 10^{-6} Pa·m^3/s depending on the length of time allowed for observation, the differential pressure applied, the lighting, background contrast and whether a pressure or vacuum is applied (Guazzo, 1994). The bubble test cannot be used as a 100% leak detection test for food packages because of package wetting (Morton, 1987).

Pressure/Vacuum Decay Testing

The pressure decay test identifies leakers by applying a pressure or vacuum to the package and then measuring the pressure change within the container. Typically a vacuum is applied. This causes the package to "balloon out" if there are no large leaks present. This test is usually used as a quick test for seal integrity and is the most common test used for on-line nondestructive leak testing (Kelsey, 1990). The sensitivity of this test method is about 10^{-5} Pa·m^3/s (Morton, 1987).

Dye Penetration Testing

The dye penetration test is a test that uses suitable dyes that penetrate surface discontinuities to enable the defect to be visible. The dye used may be either detected visually, by microscopy, or by UV illumination. Typically, the dye powder is solubilized in a solvent of low surface tension and viscosity. This allows the dye to rapidly penetrate the leak by capillary action. The package can either be submerged in the dye solution and pulling a vacuum or imposing a pressure (Morton, 1987), or the dye can be applied to the outside of the package in a suspected leakage area. Another dye test sometimes used is to inject the dye into the package and allow it to settle to the lowest edge of the container, then the dye will flow into a defect by liquid static head pressure (Hackett, 1996).

The dye test is considered a qualitative test, although it has been reported to have a sensitivity of 10^{-7} Pa·m^3/s (Morton, 1987). This may be too sensitive of a test if it is being used to detect packages that may lose their hermetic seal. Theoretically, microbial penetration should not occur if the leakage rate is below 10^{-5} Pa·m^3/s (Guazzo, 1994).

The high sensitivity can be obtained by adding a detergent that lowers the surface tension of the dye solution. A common detergent used is Triton X-100 at a concentration that does not exceed its critical micelle formation concentration. This is the point at which increasing the concentration of detergent does not further decrease the surface tension (Hackett, 1996).

Chemical Tracer Testing

This test is similar to the dye penetration test, in that a chemical solution is applied to one side of the package then tested for on the other side. These tests are more sensitive than a dye test because detection techniques as sensitive as HPLC can be used. Short-lived radionuclides such as technetium 99 and chromium 51 have also been used for sensitive leak detection experiments (Butler et al., 1977)

Electroconductivity and Capacitance Testing

This method involves applying a high frequency voltage to the package. Any liquid in a defect will increase the conductivity of the electricity. It is claimed to detect pinholes down to 0.5 μm diameter (Guazzo, 1994). An electrical capacitance test functions in much the same way. A small electrical charge is applied to the container, any liquid present in a defect results in a greater dielectric constant reading than if no liquid was present (Guazzo, 1994).

Helium Leak Testing

Gas leak detection tests are similar to the chemical tracer tests. The gas is applied to one side of the container and is probed for on the other side. The gas test is much more sensitive than a liquid test. Helium is the only gas that can leak through the smallest of defects. It is so sensitive that it can sometimes be confused with diffusion of helium through a material (Guazzo, 1994).

A leak test method using hydrogen as a tracer gas was used to detect microholes down to at least 10 μm which was the lowest size microhole used in the experiment (Hurme et al., 1998). It was also shown that the sensitivity and testing speed can be

increased if the concentration of hydrogen is increased. Using helium as a leak detection method, micro-sized holes down to at least 1 μm were detected (Gilchrist et al., 1985). The high sensitivity of the helium test method should be able to predict nano-sized holes.

Ultrasonic Leak Testing

Ultrasonic leak testing is done with a device that directs high frequency soundwaves into the package material. Any discontinuity on the surface and subsurface will cause the soundwave to be reflected. It has been said that the ultrasonic leak testers can detect a leakers down to at least 1 μm diameter (Jarrosson, 1992). Since this test makes use of soundwaves, the ultrasonic detection is the speed of sound, the testing speed, of an entire package, is limited by the scanning equipment speed and the size of the package (Jarrosson, 1992).

MICROBIAL CHALLENGE TESTING

Microbial challenge testing indicates the possibility of microbial contamination. Containers filled with product or culture media are exposed to microorganisms and then evaluated for sterility. Microbial challenge tests are obviously destructive, and could never be used to test a package before sending it out to a consumer. There are three basic variations of microbial challenge tests: immersion, static ambient, and bioaerosol (Guazzo, 1994).

The microbial challenge test is what has been used in many studies to determine conditions for post-process contamination and critical leak size (Anema and Schram, 1980; Bankes and Stringer, 1988; Chen et al., 1991; Hurme et al., 1997; Gilchrist et al., 1989; Keller, 1998; McEldowney et al., 1988; McEldowney and Fletcher, 1990; Michels and Schram, 1979; Put et al., 1972; Put et al., 1980; Stersky et al., 1980; Blakistone et al., 1996; Keller et al., 1996).

Immersion Biotesting

Immersion biotesting consists of immersing a suspect leaker into a temperature controlled water bath that contains a high concentration of indicator microorganisms. The concentration of test organisms can be greater than 10^8 CFU/ml (Guazzo, 1994; Keller, 1998; Jarrosson, 1992;). This concentration would never be found bombarding the package during its normal shelf life. Therefore the immersion test is not a real world scenario. Leakers are usually pre-screened for the immersion biochallenge by a simple bubble test (Put et al., 1980).

Static Ambient Biotesting

Static ambient tests involve placing the product or media-filled packages in storage and evaluating them over time for sterility. This is typically performed using packaged culture media taken from the filling validation run for an aseptically filled product (Guazzo, 1994). This type of biotest is the most similar to the conditions that a package may encounter during its shelf life, however, it is not practical because of its time consumption. However, in order to mimic the actual conditions a static ambient test was done over the course of 7 - 14 days to determine sensory and microbial distribution within aseptic packages containing artificial pinholes of 0.2 - 0.3 mm diameter (Kamei, 1991).

Bioaerosol Testing

A newer test method that more closely represents conditions that a package might experience is the spray cabinet, bioaerosol exposure method (Reich, 1985; Placencia et al., 1986; Chen et al., 1991; Guazzo, 1994; Keller et al., 1995, 1996, 1998). Bioaerosol testing is swiftly moving to replace immersion biotesting. The bioaerosol represents a closer match to the conditions that an aseptic package would face during its shelf life than the immersion test (Blakistone et al., 1996; Guazzo, 1994).

A bioaerosol test is a test intended to mimic conditions that are typically encountered by a package. A spray cabinet exposure chamber is used for the biotest. In

this spray cabinet is placed the sample. Then a suspension of bacteria at a known concentration is aerosolized into the exposure chamber. It is important for the bacteria to be evenly distributed throughout the exposure chamber to assure that all test surfaces of the sample are bombarded by the same amount of bioaerosol. The method of bioaerosol exposure used in this research is the dispersion of an aerosol of mean particle size 2.68 μm containing 10^6 CFU/ml motile *Pseudomonas fragi* Lacy-1052 into a test chamber of 6,125 cm^3 for a period of 35 min (Keller, 1998).

BIOAEROSOLS

Bioaerosols, as defined by the American Conference of Governmental Industrial Hygienists, are airborne particles, large molecules or volatile compounds that are living, contain living organisms or were released from living organisms (Kowalski et al., 2000). This definition includes pollen, spores, viruses, and bacteria. Since these are the main types of living organisms that comprise bioaerosols, the size range of bioaerosols typically falls between 0.01 μm to 100 μm diameter.

Bacteria can replicate while in a bioaerosol droplet (Dimmick et al., 1979). This is not a large concern for this research because there is not enough time in the test to allow replication. When the aerosol particle is approximately 4 - 6 μm, more than one cell division occurred (Dimmick et al., 1979). The median aerodynamic particle size of bioaerosols collected at a wastewater spray irrigation site was measured at 5 μm (Bausum et al., 1982).

Bioaerosols are found in nature at low concentrations. However, there are conditions that may increase the concentration of pathogenic organisms in the bioaerosol mixed microbial population. Enteric microorganisms have been detected by air monitoring procedures as far as 1,200 m from a wastewater treatment facility (Teltsch et al., 1980). Also, there has been an increased incidence of enteric disease among residents who reside in close proximity to a sewage treatment plant. This has been associated with bioaerosols emanating from the wastewater treatment plant (Teltsch et al., 1980).

The bioaerosol concentrations in swine and poultry confinement areas was found to be as high and sometimes higher than the concentrations found at a wastewater treatment plant (Clark et al., 1983). Bioaerosols also have the ability to travel great distances in air currents. Bacterial spores from the Black Sea area were found as far away as Sweden and Finland (Bovallius et al., 1978).

In a food processing plant, bioaerosol concentrations can increase quite sharply due to various processing methods used. A study in 1982 found that airborne levels of bacteria at a poultry plant shackling line reached up to $6.5x10^5$ cfu/m^3 (Lenhart et al., 1982). Bioaerosol levels of bacteria in a food processing plant operating with concurrent sanitation were measured to be 850 to 2500 cfu/m^3. This was almost 10 times greater than the plate counts for the production alone without concurrent sanitation. It was believed that sanitation pressure washing was the major cause for the elevated levels of bioaerosols (Sheehan and Giranda, 1994).

Bioaerosol Particle Size

The size of bioaerosol particles is generally indicated by an average or median diameter. With an air flow of 8 L/min and the nebulizer set-up with all ports closed, the mass median aerodynamic diameter of the particles is 2.68 μm. The radius is half of that, 1.34 μm, and, using the equation for volume of a sphere, the volume of the particle is 10.08 μm^3. The density of a typical bioaerosol particle is approximately 1.1 g/ cm^3 from which the mass of the particle can be calculated at 1.11×10^{-11}g.

The bioaerosol particle is being considered a sphere for the basic calculations necessary to predict the impact of a particle on the microtube opening. Most of the theory used in aerosol particle physics is based on the assumption that the particle is spherical (Leith, 1987; Hoppel and Frick, 1986). For aerosol particles, however, most are not spheres. Among the shapes that are easiest to define, one might find and aerosol particle in the shape of spheroids, needles, lenses, hemispheres, hollow spherical caps, toroids, and rods; however, it has been said that most aerosols found in nature actually have much more indescribable shapes. These intricate shapes make it impossible to calculate the exact behavior of these particles (Leith, 1987). That is why, in this paper, the bioaerosol

particles are being considered as spheres for the purpose of a ball-park prediction of impact probability.

Bioaerosol Particle Behavior

An aerosol is a system of small particles dispersed throughout a gaseous phase. There are many mathematical explanations of aerosol behavior that can predict the nature of the aerosolized particle. These calculations are quite tedious and are beyond the scope of this research. However, the basic calculations are used to give a ball-park probability of impact of a bioaerosol particle on the microtube opening.

To determine what kind of basic kinetics an aerosol particle may have, a benchmark, unitless number, the Knudsen number, was developed. Very small particles have Knudsen numbers that are greater than 1.0 and larger aerosol particles, such as bioaerosols, have Knudsen numbers that are far below 1.0. When the Knudsen number is as small as it typically is for bioaerosols (Gnanasekharan and Floros, 1995; Kowalski et al., 2000), the particle diameter is much greater than the mean free path. The Knudsen number is the ratio of the mean free path (λ) and the radius of the particle ($\mathbf{R_p}$).

$$\mathrm{Kn} = \frac{\lambda}{\mathrm{R_p}} \qquad \{15\}$$

The mean free path is the average distance between collisions for gas molecules or the much larger aerosol particles. The calculation takes into account the average relative velocity between the particles, which is $\sqrt{2}$ times the amount of collisions achieved than if the target particle were stationary. The mean free path equation depends on the temperature (**T**, in Kelvins) and pressure (**P** in kPa) as well as the particle diameter (**d** in meters). The universal gas constant, **R**, has a value of 8.3145 J/mol·K and Avogadro's Number, $\mathbf{N_A}$, is 6.0221 x 10^{23} particles/mol (Nave, 2000).

$$\lambda = \frac{R\mathrm{T}}{\sqrt{2}\pi d^2 N_A P} \qquad \{16\}$$

BASIC MECHANICS OF BIOAEROSOL MOVEMENT

Brownian Motion

Brownian motion is the movement of micro-particles in an irregular path. Albert Einstein explained Brownian motion as a response of larger suspended molecules to impacts from the moving molecules of the fluid medium (Cutnell and Johnson, 1995). For very small aerosol particles, Brownian motion is an important factor in the diffusion of the particle through the air as it settles due to gravity. This diffusion of the small particle through the air is not a straight path down, due to the Brownian motion.

Many of the initial studies of larger aerosol particle deposition neglect the influence of inertia as well as Brownian motion (Pich, 1972). Given that the size of bioaerosols is larger than most other aerosolized particles, Brownian motion does not play a major role in the particle's diffusion through the air, therefore it is neglected in the impact probability calculations. The behavior of bioaerosols is described as transport due to gravitational settling, thermophoresis, and turbulent convection.

Thermophoresis

Movement of bioaerosols can also be caused by thermal gradients. Particles can move from high temperatures to low temperatures (Keller, 1998). Since the bioaerosol exposure chamber is equilibrated to room temperature and the bioaerosol itself is room temperature, there is no noticeable diffusion due to a temperature gradient because there is simply no temperature differences in the chamber.

Turbulent Convection

Turbulent convection occurs when a bioaerosol particle may break out of the laminar flow of air due to a curved or angled surface (Kowalski et al., 2000). This type of diffusion is not being considered in the impact probability because the impact probability is being calculated as if the conditions are stagnant. The reason is because the concentration of bioaerosol in the exposure chamber takes 30 min to reach the target

concentration of 10^6 CFU/cm^3, followed by a 5 min period of no bioaerosol influx. The change in concentration during the initial 30 min cannot be easily added into the equations. Since a ball-park figure is all that is required the initial 30 min increasing concentration is being added to the 5 min stagnant concentration yielding the concentration of bioaerosol to be estimated at 10^6 CFU/cm^3 for 30 min.

Gravitational Sedimentation

Gravitational sedimentation is the transport due to gravity. This is the main factor affecting the bioaerosol particles in the exposure chamber. Assuming laminar flow conditions and using Stoke's law, the equation to determine the gravitational settling velocity ($\mathbf{V_{gs}}$ in cm/s) is (Gnanasekharan and Floros, 1995):

$$V_{gs} = \frac{m_p g}{6\pi R_p \mu_{air}} \qquad \{17\}$$

Where $\mathbf{R_p}$ is the radius of the bioaerosol particle (1.34 μm), μ_{air} is the viscosity of air (1.85 x 10-5 kg/m·s), **g** is the acceleration due to gravity (9800 cm/s^2), and $\mathbf{m_p}$ is the mass of the bioaerosol particle (1.11 x 10^{-11}g). These factors result in a gravitational settling velocity of 0.02 cm/s. This number can be converted to 8 x 10^{-6} cm^3/s and since there are approximately 10^6 cfu/cm^3, that is a sedimentation rate of 8 cfu/s or 0.125 s/cfu. The exposure section is 7 cm in height, and the microtubes, on average, extend 1 cm from the floor of the exposure section. This means that it will take 300 s (5 min) for the topmost particles to fall to the bottom where the microtubes are situated.

PROBABILITY OF BIOAEROSOL ENTERING MICROTUBE

Diffusive Flux of Bioaerosol in Still Air

The diffusive flux in stagnant air conditions of a particle down a microtube was calculated to be 2 x 10^{-6} CFU/s. This number is quite low considering that if the inverse is taken, then it would take 5 x 10^{5} s/CFU for one particle to move down a microtube of 7 mm length by 50 μm diameter. The calculation of the diffusive flux is according to Fick's Law (Davis, 2000).

$$N_A = -D\frac{\Delta C}{\Delta L} \qquad \{18\}$$

Where ΔC is the difference in concentration of bacteria in the exposure chamber and in the microtube. Since one bacteria is all that is needed in the microtube for sterility compromise, ΔC is 10^{6} CFU. The ΔL is the length of the microtube (7 mm). The diffusion coefficient of the bioaerosol particle in still air, *D*, is calculated using viscosity, μ, the radius of the microtube, R, and kT being equal to 4.11 x 10^{-4} J/mol,

$$D = \frac{kT}{6\pi\mu R} \qquad \{19\}$$

Convection of Bioaerosol Particle due to Air Flow

The major factor involved in the initial ingress of one bioaerosol particle is the air speed that the vacuum is pulling through the microhole, $\mathbf{Q_{air}}$. These velocities are quite low considering the microscopic sizes of the microtube diameters. The calculation is based on the Hagen-Poiselle volumetric flow rate equation {3} where the viscosity term, **μ**, is the viscosity of air (1.85 x 10^{-5} kg/m·s, which is equal to 1.85 x 10^{-5} Pa·s) and the

pressure differential, $(P_o - P_L)$, is the imposed vacuum in pascals. The number of bacteria that this air flow rate can pull into the microtube, M_B in CFU/s, is calculated as

$$M_B = Q_{air} \cdot C_B \quad \{18\}$$

Where C_B is the concentration of bacteria, 10^6 CFU/cm^3. The inverse of this number equals the number of seconds that it takes for one bacteria to enter the microtube, t^* (s/CFU). Table 1 shows how many seconds are required for one CFU to impact upon the microtube hydraulic diameter due to the air flow into the microtube caused by pulling a vacuum of magnitude 6.9, 13.8, and 34.5 kPa. The equilibrium pressure (0 kPa) mathematically shows zero impaction due to air flow, because there is no air flow at exactly 0 psi. The actual pressure differential may be slightly higher or lower due to pressure fluxuations (± 0.42 kPa) in the exposure chamber.

Table 1 – Number of seconds required for one bacteria, (s/CFU), to impact the microtube of hydraulic diameter due to air-flow into the microtube caused by pulling a vacuum of 6.9, 13.8, or 34.5 kPa.

	IMPOSED VACUUM		
Hydraulic Diameter (μm)	**-6.9 kPa (s/CFU)**	**-13.8 kPa (s/CFU)**	**-34.5 kPa (s/CFU)**
2	4.8E+01	2.4E+01	9.6E+00
5	1.2E+00	6.1E-01	2.5E-01
7	3.2E-01	1.6E-01	6.0E-02
10	8.0E-02	4.0E-02	2.0E-02
20	4.8E-03	2.4E-03	9.6E-04
50	1.2E-04	6.1E-05	2.5E-05

REFERENCES

Amini, M. A., and D. R. Morrow. 1979. Leakage and permeation: theory and practical applications. Package Dev. and Sys. May/June: 20-27.

Anderson, G. L. 1989. Leak testing. p.50-57. *In* 9th ed. Nondestructive evaluation and quality control: metals handbook. AOAC, Arlington, VA.

Anema, P. J., and B. L. Schram. 1980. Prevention of post-process contamination of semi-rigid and flexible containers. J. Food Prot. 43(6):461-464.

Anonymous. 1982. Leak Testing. *In* Nondestructive testing handbook, vol. 1. American Society for Nondestructive Testing, American Society for Metals.

Anonymous. 1998. An interview with Clifford M. Coles: advantages of sterility testing for aseptically processed foods. Food Testing & Analysis. Aug-Sep, 1998.

ASTM. 2000. Standard terminology for nondestructive examinations. standard no. E1316-99a. *In* American Society for Testing and Materials. West Conshohocken, PA.

Bankes, P., and M. F. Stringer. 1988. The design and application of a model system to investigate physical factors affecting container leakage. Int. J. Food Micro. 6:281-286.

Bausum, H. T., S. A. Schaub, K. F. Kenyon, and M. J. Small. 1982. Comparison of coliophage and bacterial aerosols at a wastewater spray irrigation site. Appl. Environ. Microbiol. 43(1):28-38.

Blakistone, B. A., S. W. Keller, J. E. Marcy, G. H. Lacy, C. R. Hackney, and W. H. Carter, Jr. 1996. Contamination of flexible pouches challenged by immersion biotesting. J. Food Prot. 59(7):764-767.

Bovallius, A., B. Bucht, R. Roffey, and P. Anas. 1978. Long-range air transmission of bacteria. Appl. Environ. Microbiol. 35(6):1231-1232.

Bryant, M. 1988. Packaging failures: quality in design doesn't end with the finished product. Med. Dev. & Diag. Ind. 10(8):30-33.

Butler, L. D., J. J. Coupal, and P. P. DeLuca. 1978. The detection of ampul leakers using short-lived radionuclides. Journal of the Parenteral Drug Association. 32(1): 2-9.

Chen, C., B. Harte, C. Lai, J. Pestka, and D. Henyon. 1991. Assessment of package integrity using a spray cabinet technique. J. Food Prot. 54(8):643-647.

Clark, S. R. Rylander, and L. Larsson. 1983. Airborne bacteria, endotoxin and fungi in dust in poutry and swine confinement buildings. Am. Ind. Hyg. Assoc. J. 44(7):537-541.

Cutnell, J. D., and K. W. Johnson (ed.). 1995. Physics 3rd ed. John Wiley and Sons, Inc. New York.

Davidson, P. M., and I. J. Pflug. 1981. Leakage potential of swelled cans of low-acid foods collected from supermarkets. J. Food. Prot. 44(9):692-695.

Davis, R. M. 1999. Personal Communication. Associate Professor, Chemical Engineering, Virginia Polytechnic Institute and State University, Blacksburg, VA.

Davis, R. M. 2000. Personal Communication. Associate Professor, Chemical Engineering, Virginia Polytechnic Institute and State University, Blacksburg, VA.

Dimmick, R. L., H. Wolochow, and M. A. Chatigny. 1979. Evidence for more than one division of bacteria within airborne particles. Appl. Environ. Microbiol. 38(4):642-643.

Eisenberg, D., and D. M. Crothers. 1979. Physical chemistry with applications to the life sciences. p.726. Benjamin/Cummings Publishing Co. Menlo Park, CA.

Gilchrist, J. E., U. S. Rhea, R. W. Dickerson, and J. E. Campbell. 1985. Helium leak test for micron-sized holes in canned foods. J. Food Prot. 48(10):856-860.

Gilchrist, J. E., D. B. Shah, D. C. Radle, and R. W. Dickerson, Jr. 1989. Leak detection in flexible retort pouches. J. Food Prot. 52(6):412-415.

Gnanasekharan, V., and J. D. Floros. 1995. A theoretical perspective on the minimum leak size for package integrity evaluation. p.55-65. *In* B. A. Blakistone, and C. L. Harper (eds.). Plastic package integrity testing - assuring seal quality. IOPP. Herndon, VA.

Goode, Jr., J. E., and A. M. Souter. 1995. Rancidity in Packaged nuts: end-use technical service. J. Plastic Film and Sheeting. 11(7):235-247.

Guazzo, D.M. 1994. Package Integrity Testing, p. 247-276. *In* M. J. Akers (ed.), Parenteral quality control: sterility, pyrogen, particulate, and package integrity testing, 2nd ed Mercel Dekker, New York.

Hackett, E. T. 1996. Dye penetration effective for detecting package seal defects. Packag. Tech. Eng. 8:49-52.

Harper, C. L., B. A. Blakistone, J. B. Litchfield, S. A. Morris. 1995. Developments in food packaging integrity testing. Trends in Food Sci. and Technol. 6(10):336-340.

Hoppel, W. A., and G. M. Frick. 1986. Ion-aerosol attachment coefficients and the steady-state charge distribution on aerosols in a bipolar ion environment. Aerosol Sci. and Technol. 5:1-21.

Howard, G., and R. Duberstein. 1980. A case of penetration of 0.2 mm rated membrane filters by bacteria. J. Parenter. Drug Assoc. 34(2):95-102.

Hurme, E. U., G. Wirtanen, L. Axelson-Larsson, N. A. M. Pachero, and R. Ahvenainen. 1997. Penetration of bacteria through microholes in semirigid aseptic and retort packages. J. Food Prot. 60(5):520-524.

Hurme, E. U., and R. Ahvenainen. 1998. A nondestructive leak detection method for flexible food packages using hydrogen as a tracer gas. J. Food Prot. 61(9):1165-1169.

Jarrosson, B. P. 1992. Closure integrity testing of heat sealed aseptic packaging using scanning acoustic microscopy. M.S. Thesis, Virginia Polytechnic Institute and State University, Blacksburg, VA.

Kamei, T., J. Sato, A. Natsume, and K. Noda. 1991. Microbiological quality of aseptic packaging and the effect of pinholes on sterility of aseptic products. Pack. Technol. and Sci. 4:185-193.

Keller, S., J. E. Marcy, B. A. Blakistone, and G. H. Lacy. 1995. Package integrity biotesting: aerosol versus immersion. *In* T. Ohlsson (ed.). Proceedings of the International Symposium Advances in Aseptic Processing and Packaging Technologies. SIK, Goteborg, Sweden.

Keller, S., J. E. Marcy, B. A. Blakistone, G. H. Lacy, C. R. Hackney, and W. H. Carter, Jr. 1996. Bioaerosol exposure method for package integrity testing. J. Food Prot. 59(7):768-771.

Keller, S. 1998. Determination of the leak size critical to package sterility maintenance. Ph.D. Dissertation, Virginia Polytechnic Institute and State University, Blacksburg, VA.

Kelsey, R. J. 1990. The status of leak detection. Food and Drug Pack. 11:8-21.

Kowalski, W. J., W. P. Bahnfleth, and T. S. Whittam. 2000. "Bioaerosols and bioaerosol dynamics," (Aerobiological Engineering at The Pennsylvania State University), [Internet, WWW], ADDRESS: http://www.engr.psu.edu/www/dept/arc/server/WJKAEROB.HTML

Lake, D. E., R. R. Graves, R. S. Lesniewski, and J. E. Anderson. 1985. Post-processing spoilage of low-acid canned foods by mesophilic anaerobic sporeformers. J. Food Prot. 48(3):221-226.

Lampi, R. A. 1980. Retort pouch: the development of a basic packaging concept in today's high technology era. J. Food Process Eng. 4:1-18.

Lee, Y. K., and K. Hoon. 1995. "Surprise 95-brownian motion-the research goes on," [Internet, WWW], ADDRESS: http://www-dse.doc.ic.ac.uk/~nd/surprise_95/journal/vol4/ykl/report.html

Leith, D. 1987. Drag on nonspherical objects. Aerosol Sci. and Technol. 6:153-161.

Lenhart, S. W., S. A. Olenchock, and E. C. Cole. 1982. Viable sampling for airborne bacteria in a poultry processing plant. J.Toxicol.Environ.Health. 10:613-619.

Loeb, L. B (ed.). 1961. The kinetic theory of gases, 3rd ed. p. 278-300. Dover Publications, New York.

McEldowney, S., and M. Fletcher. 1988. Bacterial desorption from food container and food processing surfaces. Microb. Ecol. 15:229-237.

McEldowney, S., and M. Fletcher. 1990a. A model system for the study of food container leakage. J. Appl. Bacteriol. 69:206-210.

McEldowney, S., and M. Fletcher. 1990b. The effect of physical and microbiological factors on food container leakage. J. Appl. Bacteriol. 69:190-205.

Michels, M. J. M., and B. L. Schram. 1979. Effect of handling procedures on the post-process contamination of retort pouches. J. Appl. Bacteriol. 47:105-111.

Morris, S. A., A. Ozguler, and W. D. O'Brien, Jr. May 21, 1999. "New sensors help improve heat-seal microleak detection." (Packaging Technology and Engineering Feature). [Internet, WWW]. ADDRESS: http://www.napco.com/pte/0798sensors.html.

Morton, D. K. 1987. Container/closure integrity of parenteral vials. J. Parenter. Sci. Technol. 41(5):145-158.

Morton, D. K., N. G. Lordi, L. H. Troutman, and T. J. Ambrosio. 1989. Quantitative and mechanistic measurements of container/closure integrity: bubble, liquid, and microbial leakage tests. J. Parenter. Sci. Technol. 43:104-108.

Nave, C. R. 2000. "Mean free path and refinement of mean free path," (Hyperphysics, Department of Physics and Astronomy at Georgia State University), [Internet, WWW], ADDRESS: http://www.230nscl.phy-astr.gsu.edu/hbase/kinetic/menfre.html

Pflug, I. J., P. M. Davidson, and R. G. Holcomd. 1981. Incidence of canned food spoilage at the retail level. J. Food Prot. 44(9):682-685.

Pich, J. 1972. Theory of gravitational deposition of particles from laminar flows in channels. J. Aerosol Sci. 3:351-361.

Placencia, A. M., G. S. Oxborrow, and J. T. Peeler. 1986. Package integrity methodology for testing the biobarrier of porous packaging. part II: FDA exposure-chamber method. Med. Dev. & Diag. Ind. 8(4)46-53.

Put, H. M. C., H. T. Witvoet, and W. R. Warner. 1980. Mechanism of microbiological leaker spoilage of canned foods: a review. J. Appl. Bacteriol. 35:7-27.

Put, H. M. C., H. T. Witvoet, and W. R. Warner. 1980. Mechanism of microbiological leaker spoilage of canned foods: biophysical aspects. J. Food Prot. 43(6):488-497.

Reich, R. R. 1985. A method for evaluating the microbial barrier properties of intact packages. Med. Dev. and Diag. Ind. 7(3):80-88.

Sheehan, M. J., and J. V. Giranda. 1994. Bioaerosol generation in a food processing plant: a comparison of production and sanitation operations. Appl. Occup. Environ. Hyg. 9(5):346-352.

Stauffer, T. 1990. Non-destructive testing on flexible packaging. J. pack. Technol. July/August:27-29.

Stersky, A., E. Todd, and H. Pivnick. 1980. Food poisoning associated with post process leakage (PPL) in canned foods. J. Food. Prot. 43(6):465-476.

Teltsch, B., H. I. Shuval, and J. Tadmor. 1980. Die-away knetics of aerosolized bacteria from sprinkler application of wastewater. Appl. Environ. Microbiol. 39(6):1191-1197.

Thompson, P. J., and M. A. Griffith. 1983. Identity of mesophilic anaerobic sporeformers cultured from recycled cannery cooling water. J. Food Prot. 46(5):400-402.

Whitaker, S. (ed.). 1992. Introduction to fluid mechanics, p. 21. Krieger Publishing Company. Malabar, FL.

Yeh, H. J., and A. Benatar. 1997. Technical evaluation: methods for sealing paper/foil aseptic food packages. TAPPI Journal. 80(6):197-203.

SECTION II

ABSTRACT

Threshold leak sizes and leak rates were calculated for a number of liquid food products exhibiting a wide range of surface tension and viscosity values. From this data, it can be seen that mathematically, under typical pressure differentials generated in food packages (≤ ±34.5 kPa), a leak will not start through a 2 μm defect. The calculated leak rates were compared to calculated evaporation rates of pure water. The evaporation rate exceeds the leak rate at lower sized microholes (2 and 5 μm diameter) under typical pressure differentials found in food packages. If the liquid, typically aqueous in food products, is evaporating off faster than the leak itself, then there will be solids left behind that could effectively plug the leak.

The critical leak size is the size micro-defect that allows microbial penetration into the package. The critical leak size of air-filled defects was found to be 7 μm at all pressures tested. This size is considerably important to food packagers because this is when sterility of the package is lost. Previous leak studies have shown that the critical leak size for liquid-filled defects coincide with the threshold leak size and pressure. If this is in fact true, then air-filled defects should exhibit a larger critical leak size than the liquid-filled defects. In this study, air-filled defects were examined. A bioaerosol exposure chamber was used to test micro-defects, nickel microtubes of known diameters 2, 5, 7, 10, 20, and 50 μm hydraulic diameters, against pressure differentials of 0, -6.9, -13.8, and -34.5 kPa.

INTRODUCTION

Package integrity testing has been the focus of significant interest to the flexible and semi-rigid packaging industry. It would be ideal for the industry to reach the same levels of sterility maintenance assurance that has been reached for cans (*6*). More companies are moving towards a 100% on-line nondestructive leak test that assures all containers leaving the facility to be sterile. Leak testing in this manner ultimately decreases the overall costs by reducing the number of reworked or recalled products (*2, 53, 54*). In order for an on-line leak tester to be efficient, the minimum leak size that is critical to microbial ingress must be scientifically established (*21*).

Nondestructive leak testing equipment relies on physical testing methods because of their fast test speed, reliability, and repeatability. Most of the on-line leak testing equipment are base on a variation of the pressure decay test (*33*). A package is enclosed in an air- tight chamber, the air around the package is evacuated, and a pressure-transducer system measures any change in the package internal pressure. Ultrasonic leak detection equipment is becoming very favorable to food packagers because it can detect leaks at least as small as 1 μm and operates at the speed of sound (*27, 33*). There are other laboratory physical tests that are even more sensitive such as the tracer gas leak and helium leak test (*18, 19, 43*). Dye penetration tests, chemical tracer tests, and bubble tests are the most popular destructive leak tests performed in the laboratory (*4, 18, 19, 20, 43*).

A physical test alone, however, does not indicate if the package's sterility can been breached (*6, 9, 17, 18, 21, 29, 31, 52*). The efficiency of a physical test must be compared to that of a microbial biotest to indicate the conditions under which a package will become susceptible to microbial contamination (*6, 9, 21, 29, 31, 52*).

The immersion biotest is a widely used method of determining if a package is leaking to the extent of allowing microbial infiltration. The number of bacteria in the immersion media affects the number of packages that will be contaminated (*3, 7*). Typically, concentrations of bacteria in the immersion broth can be upwards of 10^9 CFU/ml (*31*). A package would never encounter this great a bacterial concentration

during its normal shelf life. An aseptic package will never be exposed to a liquid bath like a retortable package (*6*).

In order to more closely mimic conditions encountered by an aseptic package, a bioaerosol exposure test method has also been employed (*12, 29, 30, 31, 46, 50*). The contact of an aseptic package by microorganism is going to be through aerosolized particles in the air (*6*). Bioaerosols have become more prominent in the eyes of scientific researchers as of late because of their potential of carrying pathogenic organisms. Many studies have been done at wastewater treatment plants and farms that show that aerosolized bacteria can in fact be hazardous to humans and animals (*13, 56*), carried great distances through air currents (*8, 56*), and can replicate more than once in particles of average size (*5, 16*). Levels of bioaerosol found at a poultry plant shackling line have reached up to $6.5x10^5$ CFU/m^3 (*37*). Bioaerosol levels of bacteria in a food processing plant operating with concurrent sanitation were measured to be 850 to 2500 CFU/m^3 (*51*). Keller et al. found that using a bioaerosol chamber with 10^6 CFU/cm^3 bacteria results in faster test runs with significant differences between micro-defect diameters (30).

Research efforts have attempted to characterize conditions that lead to package spoilage. Earlier leak studies have shown that microorganisms more readily traverse defects that are filled with liquid by mechanism of motility or pressure differentials found within the leak (*1, 14, 19, 25, 28, 31, 38, 39, 43, 44, 45, 46, 47, 48, 55*). Because of the difficulty involved in manufacturing micron sized defects, many studies involved using porous membranes of known sizes (*4, 39, 40, 46, 50*).

Post-process contamination studies led to suggestions on how to avoid contamination after processing retort pouches (*41, 47, 55*). Immediately drying a container after the retort cooling process decreases the contamination rate to less than 1% (*41*). A study in 1983 showed that bacteria typically contaminating the recycled cooling water of a still retort are of the *Clostridium* species (*57*).

The critical leak size of microbial contamination has been suggested many times. It has fluctuated from being between 0.2 μm to 0.4 μm (*23*), to it being unlikely that the critical leak size is less than 10 μm (*36*), to it being less than 10 μm (*6, 7, 21, 24, 30, 31*), 10 or 5 μm (*12*), considerably larger than 1 μm (*35*), and also 1 μm under certain

conditions (*40, 46*). It has also been 22 μm (*18*), and 11 μm (*36*). There are overlaps and discrepancies both in these numbers. The critical leak size was correlated with the threshold leak size under normal pressure differentials that may be encountered in food packages (*31*). That is to say, the critical leak size is approximately the same size that allows a micro-defect to become liquid-filled.

An equation was developed to predict the threshold leak size and pressure using the surface tension of the liquid food product as the main factor involved in leak initiation through micro-sized defects (*31*). Once the leak has been initiated, the flow rate and evaporation rate become factors in leakage. If the flow rate is faster than the evaporation rate, then leakage will occur. If the flow rate is below the evaporation rate, then it is believed that soluble solids will plug the microhole (*15, 31*).

The first objective of this research was to quantify threshold leak pressures and leak rates for liquid food products with a wide range of surface tensions, viscosities, densities, and package size. This will allow the threshold leak size to be calculated for typical internally generated pressures in the package.

The second objective of this research was to biotest air filled defects with a bioaerosol exposure chamber to compare threshold leak size and critical leak size. Since the critical leak size has been linked to the threshold leak size by bioaerosol testing liquid-filled defects and comparing them to the threshold leak size (*31*), it is necessary to test whether an air-filled defect will have a different critical leak size.

MATERIALS AND METHODS

Density Measurement

The densities of the liquids in this study were measured by weighing 1 ml of the liquid on an analytical balance at room temperature. The weight of the 1 ml is the density in g/ml, which can be multiplied by 1,000 to give the density in kg/m^3. The density of the liquid is used to calculate the liquid static head. These calculations yield numbers that do

not change the threshold leak pressure by more than 5% even in the largest container fill height of 20 cm. Since the density of the liquid is not of major concern for this research, the number achieved by this method is sufficient.

Viscosity Measurement

Capillary tube viscometers and rotational viscometers are the most common methods of determining the viscosity of a liquid. The research presented here makes use of a rotational viscometer.

A Brookfield LVT rotational viscometer (Brookfield Engineering Laboratories, Inc., Stoughton, MA) was used for viscosity measurements. The rotational viscometer is a cylinder inside of a slightly larger cylinder. The liquid to be tested is placed in between the large and small cylinders. The inside (smaller) cylinder is rotated at a fixed number of revolutions per minute. The viscometer measures the amount of torque required to turn the inner cylinder at the specified rpm. The inside cylinder attachment used for all samples except the corn syrup was the UL- 25 ml rotating cylinder. The corn syrup was measured using the LV2 attachment. Two different speeds were used.

Surface Tension Measurement

Surface tensions were measured using a KSV Instruments Sigma 70 (Monroe, CT) with computer interface. The machine reads the surface tension based on the du Nouy ring method of surface tension measurement. All values were corrected by the computer according to the Huh-Mason surface tension correction method. The platinum ring used was the standard ring for the Sigma 70 (R = 9.545 mm, r = 0.185 mm, Wetted Length = 119.9 mm). The vessel used to contain the test sample was the standard test vessel as indicated for the Sigma 70 (Diameter = 66 mm, Max. Volume = 110 ml). The amount of liquid used was between 80 - 100 ml per sample. The density of each sample is entered into the computer before each run. The Sigma 70 constantly measures the temperature of the room.

Threshold Leak Equation

To predict the threshold leak pressures of various package defects, a mathematical model was developed by Keller (*31*). This equation predicts the (imposed) pressure, $\mathbf{P_o}$ (in kPa), required to initiate a leak of a liquid of surface tension, $\boldsymbol{\sigma}$ (in mN/m), through a microhole of (hydraulic) diameter, $\mathbf{D_h}$ (in μm). The term $\boldsymbol{\rho gL}$ represents the liquid static head (in kPa), which is the density of the liquid, $\boldsymbol{\rho}$ (in kg/m^3), times the acceleration of gravity, **g** (9.8 m/s^2 on Earth), and the height, **L** (in m), of liquid above the defect in the container. The atmospheric pressure ($\mathbf{P_{atm}}$) is the pressure of the environment surrounding the package, which is 101.3 KPa (14.7 psi) at sea level.

$$P_o > P_{atm} + \left[\left(\frac{4\sigma}{D_h} - \rho gL\right) \times 0.390\right] \qquad \{1\}$$

The hydraulic diameter allows for the calculation of the diameter of holes with either circular or elliptical shapes. The equation for hydraulic diameter relates the radius **a**, in the X direction, and the radius **b**, in the Y direction.

$$D_h = \frac{2ab}{\sqrt{\frac{a^2 + b^2}{2}}} \qquad \{2\}$$

The 0.390 in the threshold leak pressure equation {1} is a unitless correction factor. This correction factor was changed from 0.272 to 0.390 due to an incorrect conversion factor in the original equation. The correction factor was used to correct the mathematical values to the experimental values obtained for the threshold leak pressure of deionized water, safranin red dye, and tryptic soy broth (*31*). It was thought that the correction factor was necessary due to the hydrophilic nature of the nickel microtubes (*31*).

In order to confirm that the threshold leak pressure equation is applicable to liquid foods of differing composition, the imposed pressure of a high salt (soy sauce) and an alcohol liquid (wine) was observed through a light microscope model BH-2 (Olympus, Lake Success, NY) equipped with video calipers model MVCO3A (Olympus, Lake Success, NY) according to Keller's method (*31*).

The equation used to obtain threshold leak pressure is derived from the Hagen-Poiselle equation of volumetric rate of flow. This equation shows the relationship between the volumetric rate of flow of a laminar liquid and the forces that cause the flow. The equation is:

$$Q = \frac{\pi (P_o - P_L) R^4}{8 \mu l} \qquad \{3\}$$

where **Q** is the volumetric rate of flow in units of volume per units of time (cm^3/s). The term **π** is the number 3.14159... The radius, **R** (in cm), of the microhole plays a major part in determining the flow rate. This is quite obvious because the radius term is to the fourth power. This creates large differences in flow rate of microholes that are only micrometers different in radius. The viscosity, **μ** (in Pa·s) and the length of the leak, **l** (in cm), decrease the flow rate as they are increased. The pressure differential that drives the leakage is the term **(P_o-P_L)**. **P_o** (in Pa) is the imposed pressure on the inside of the container while **P_L** (in Pa) is the external pressure acting on the outside of the package.

Evaporation Rate Equations

Evaporation should play a major role in the critical leak size determination for various products. Mathematically, the leak rates tend to be so small that the leak rate sometimes does not even surpass the evaporation rate of water. If this happens, it is believed that soluble solids will remain after all of the liquid has evaporated and will block the flow of liquid through the defect.

The evaporation rate of the leaking liquid is determined by the following equation:

$$W_A^{(m)} = K_{xm} \pi r^2 \left[\frac{(X_{Ao} - X_{A\infty})}{(1 - X_{Ao})} \right] \qquad \{4\}$$

Where $\mathbf{W_A^{(m)}}$ is the molar evaporation rate (in gmol/s) from a droplet of radius, **r**, surface. The radius in calculations for this paper is considered to be the same as the microhole. This results in half of a sphere to be exposed to the air for evaporation. The term, $\mathbf{K_{xm}}$ (in gmol/cm^{2}s) is the mass transfer coefficient. $\mathbf{X_{Ao}}$ represents the mole fraction of water in air at the droplet's surface, and the mole fraction of water in ambient air, from relative humidity measurements (typically 60% - 80%), is indicated by $\mathbf{X_{A\infty}}$.

$$K_{xm} = \frac{C_f D_{ABF}}{r} \qquad \{5\}$$

Where $\mathbf{C_f}$ is the moles of gas per cm^3 in film and $\mathbf{D_{ABF}}$ is the binary diffusion coefficient for air-water in film. This diffusion coefficient is used only for water evaporating into air. If a liquid food contains two volatile species, such as ethanol and water, than a much more complex terniary diffusion coefficient is needed (ethanol-water-air). The complexity goes far beyond the scope needed for this research, however, the aqueous evaporation rate can be considered a lower bound because the evaporation rate of the terniary system will be faster (*15*).

The $\mathbf{C_f}$ is an estimation assuming conditions of room temperature.

$$C_f = \frac{n}{V} = \frac{P}{RT} \qquad \{6\}$$

The estimation of the binary diffusion coefficient $\mathbf{D_{ABF}}$ of water in air is

$$D_{ABF} = a\left[\frac{T}{\sqrt{T_{CA}T_{CB}}}\right]^{b}\left(P_{CA}P_{CB}\right)^{1/3}\left(T_{CA}T_{CB}\right)^{5/12}\left[\frac{1}{M_A}+\frac{1}{M_B}\right]^{1/2} \quad \{7\}$$

Where $\mathbf{a}$ = 3.64 x 10^{-4} and $\mathbf{b}$ = 2.334 for water with a nonpolar gas. $\mathbf{T}$ is the room temperature, $\mathbf{T_{CA}}$ is 132 K for air, $\mathbf{T_{CB}}$ is 647 K for water, $\mathbf{P_{CA}}$ is 36.4 atm for air, $\mathbf{P_{CB}}$ is 217.7 atm for water, $\mathbf{M_A}$ is 28.97 g/mol for air, and $\mathbf{M_B}$ is 18 g/mol for water.

$$X_{Ao} = \frac{P_w}{P_{atm}} \quad \{8\}$$

$$X_{A\infty} = \frac{H_R P_w}{100 \cdot P_{atm}} \quad \{9\}$$

Where $\mathbf{P_w}$ is the vapor pressure of water, $\mathbf{P_{atm}}$ is the atmospheric pressure, and $\mathbf{H_R}$ is the relative humidity percent (*15*).

Most liquid food products are not pure water. There are usually soluble solids or particulate matter in the mixture. Any particulate matter that is larger than the microhole may actually plug the hole. This is merely a probability problem. Soluble solids, on the other hand, may plug the hole after the water has evaporated leaving a plug behind in the hole. This raises the question as to the evaporation rate of a liquid containing these soluble solids. This rate can be calculated by substituting the vapor pressure of the liquid in question with the vapor pressure of water in equations 8 and 9. These vapor pressures can be found by measuring the water activity, A_w, which is a ratio of the vapor pressure of a food product (P) to the vapor pressure of pure water (P_o) at the same temperature.

$$A_w = \frac{P}{P_o} \quad \{10\}$$

In order to understand the difference in evaporation rate of pure water and a liquid food containing soluble solids, the water activity of sodium chloride solutions as well as soy sauce were measured using an Aqua Lab CX-2 (Pullman, Washington).

Materials for Bioaerosol Exposure

Glass Test Cells (Department of Food Science and Technology, Virginia Tech, Blacksburg, VA)

Septa closures and silicone/Teflon® septum 73818T-13 (Fisher Scientific, Atlanta, GA)

DAP 100% silicone rubber sealant (Dow Corning, Dayton, OH)

High Vacuum Grease (Dow Corning, Dayton, OH)

Teflon® Thread Seal Tape ½ inch width

27 gauge syringe needles

Nickel Microtubes of approximate hydraulic diameters 0, 2, 5, 7, 10, 20, and 50 μm (Phillips Laboratory, Fundamental Technology Division, Carbon Research Laboratory, Edwards Air Force Base, CA)

Light microscope model BH-2 (Olympus, Lake Success, NY)

Video calipers model MVCO3A (Olympus, Lake Success, NY)

Bioaerosol Exposure Chamber (Department of Food Science and Technology, Virginia Tech, Blacksburg, VA)

Black rubber tubing 14-158D (Fisher Scientific, Atlanta, GA)

Autoclavable plastic "Y" joints to fit black rubber tubing

Rubber Gaskets (approx. 6 cm OD x 2 cm ID)

6.9 m^3 size E compressed air cylinders

CGA 346 air flow meters (Controls Corporation of America, Virginia Beach, VA)

In-line pressure gauge HHP701-2 (Omega Engineering, Inc., Stamford, CT)

Vacuum/compressor pump ROA-P131-AA (Gast, Benton Harbor, MI)

In-line bacterial vents (0.33 μm filters) product no. 4210 (Gelman, Ann Arbor, MI)

Nebulizer kit 2D0807 (Baxter Healthcare, Toronto, Ontario, Canada)

Two autoclavable 2.54 cm ID x 3.2 cm OD x 30 cm (L) clear PVC tubing (Fisher Scientific, Atlanta, GA)

Pseudomonas fragi Lacy-1052 (Department of Plant Pathology, Physiology, and Weed Science, Virginia Tech, Blacksburg, VA)

Tryptic Soy Broth 0370-17-3 (Difco Laboratories, Detroit, MI)

Tryptic Soy Agar 0370-17-6 (Difco Laboratories, Detroit, MI)

Kanamycin (5 mg/ml stock solution-made fresh each day required)

Tetracycline (1 mg/ml stock solution-made fresh each day required)

Butterfield's Phosphate Buffer (0.25 M NaH_2PO_4, pH 6.8)

Bioaerosol Generator

Nebulizer kits model 2D0807 (Baxter Healthcare, Toronto, Ontario, Canada) with a mass median aerodynamic diameter of 2.68 μm, geometric standard 1.85 μm, and mass aerosol per minute of 1.1 μm and 4.7 μm were used to generate the bioaerosol. This type of nebulizer is referred to as a Wright compressed air nebulizer, which operates by impacting a high velocity liquid/air stream onto a baffle. This impaction aerosolizes the liquid. The cell suspension to be aerosolized is drawn into the airflow that is emitted from a 0.074 cm ID orifice. The flow is directed towards a small chamber and then forced through a 0.16 cm ID orifice after which it travels a distance of 0.116 cm where it is impinged upon an open-sided flat collector. Smaller droplets are able to make the turns, whereas the larger droplets collect on the baffle (*49*). The large droplets deposited on the baffle are forced by the airstream to the edge where they are aerosolized (*31*).

Airflow was 8 L/min. Two 6.9 m^3 size E cylinders of compressed air, each equipped with CGA 346 air flow meters (0-15 L/min range) (Controls Corporation of America, Virginia Beach, VA) were used for air supply (*31*).

Microtubes

Nickel microtubes were developed by the Phillips Laboratory, Fundamental Technology Division, Carbon Research Laboratory, Edwards Air Force Base, CA through a Cooperative Research and Development Agreement (*22*). Microtube internal diameters (IDs) were 2, 5, 7, 10, 20, and 50 μm. Solid microtubes (0 μm, ID) were used as negative controls.

Test Cells

The glass test cells have overall dimensions of 8 cm [h] X 5 cm [d]. It is a glass vial with septa lug for closure (45 mm [h] X 15 mm [d]) encased in an 85 ml glass water jacket. The vial and jacket each have one entry port and one exit port (*31*). The septum is made from silicone/ Teflon® no. 73818T-13 (Fisher Scientific, Atlanta, GA)

Preparation of the test cells

Using the method developed by Keller, 1998, the glass test cells were prepared as follows. A 27-gauge syringe needle was used to penetrate through the center of the silicon/ Teflon® septum. The microtube was inserted into the needle cavity where it was held in place while the needle was removed, thus leaving the microtube through the center of the septum. Care was taken to assure that the microtube was not bent during the process. Internal diameters, x and y, were measured using a light microscope model BH-2 (Olympus, Lake Success, NY) equipped with video calipers model MVCO3A (Olympus, Lake Success, NY). The diameters were halved to become radii a and b, respectively (*31*).

Once hydraulic diameters were confirmed by measurement, the septum containing the microtube was positioned onto the glass lug of the test cell. The lug was then wrapped with Teflon® Thread tape overlapping the top outside circular edge of the septum. The septa cap was then screwed down onto the lug. The surface around the microtube and the contact around the septum-septa cap area were sealed with DAP silicone sealer (Dow Corning, Dayton, OH) using extreme caution not to touch the top of the microtube (*31*). A volume of 4 ml of tryptic soy broth is pipetted through one of the entry ports into the center vial.

Bioaerosol Exposure Chamber

The bioaerosol exposure chamber developed by Keller, 1998, is constructed of Lexan® in dimensions of 35 cm (L) x 25 cm (W) x 25 cm (H). The internal area of the

chamber is 21,875 cm^3, and is divided into two sections: the utility section and the exposure section (*31*).

The utility section (dimensions: 35 cm x 25 cm x 18 cm (H); utility internal area = 15,750 cm^3) houses the vacuum, water input and recovery manifolds including all related tubing, vacuum and compressor tubing, and also seven test cells. There is an exit port to which a rubber tube with a bacterial vent is attached for pressure equalization during the autoclave cycle (*31*).

The neck of each test cell protrudes through one of seven 3.75 cm holes in the partition which, on the utilities section side (*31*), has a rubber gasket coated with vacuum grease on both sides in between the test cell and the Lexan® (Figs. 4 and 5). The test cells are held tightly in place using thick rubber gaskets in between the test cell and a flat metal bracket secured to the chamber with wingnuts. The test cells are attached to the vacuum/compressor tubing by black rubber tubing 14-158D (Fisher Scientific, Atlanta, GA) attached to a plastic "Y" connector (Fig. 6). There are three pieces of black rubber tubing attached to the "Y". To the top stems of the "Y" there is a tube of length 15 cm and a tube of length 11 cm. These two tubes are then attached to the inlets of the center vial of the test cell. To the bottom stem of the "Y" there is a 9 cm tube attached. A bacterial vent is attached to the other end, which is attached to the exposure chamber's vacuum/compressor tubing (*32*).

The exposure section (dimensions: 35 cm x 25 cm x 7 cm (H); exposure internal area = 6,125 cm^3) is where the test cell septum, microtube, and septa cap protrude from the utility section. There are two 1.4 cm ID, brass male and female threaded fitting entry and exit ports with O-ring seals, one on each opposing width panels for bioaerosol delivery and one exit port with bacterial vent used for pressure equalization (*31*).

The bioaerosol exposure chamber panels were then attached. It was then flipped upside-down, so that the exposure section was at the top and the utilities section at the bottom, and put into an autoclave for 55 min, 3 min dry time. The exposure chamber was then removed from the autoclave and cooled down overnight so that it equilibrated with the room temperature of 22-23ºC (*31*).

Test Organism

Pseudomonas fragi Lacy-1052, obtained from the library of the Department of Plant Pathology, Physiology, and Weed Science, Virginia Tech, Blacksburg, VA was used as the test (indicator) organism. This genus is aerobic, gram-negative, motile, nonsporeforming, catalase-positive rods with polar flagella. Their size ranges from 0.5 - 1.0 μm diameter and 1.5 - 5.0 μm length. Optimal temperature range for growth is from 25°C - 35°C and the optimal pH range is pH 6.6 - 8.5. This particular strain can be differentiated by kanamycin (30 μg/ml) and tetracycline (10 μg/ml). Kanamycin and tetracycline resistance are incorporated into the genome of this organism via a *Tn5* transposon (*34*). Since the antibiotic resistance genes are on the genome, selective pressure does not have to be present at all times. This is important because during the test, there is about 2 hrs where the bacteria are not in antibiotics.

Bioaerosol Preparation

Pseudomonas fragi Lacy-1052 were grown to 10^9 CFU/ml in 100 ml tryptic soy broth containing 30 μg/ml kanamycin and 10 μg/ml tetracycline (*31*). Cells were then centrifuged in a high-speed RC-5B (Sorvall Instruments, Newton, CT) at 10,000 x g for 10 min. The tryptic soy broth was aseptically replaced by 100 ml sterile Butterfield's phosphate buffer (0.25 M KH_2PO_4) that had been adjusted to pH 6.8 - 7.0 (*26*). The bacteria were then resuspended by vortexing and transferred to the reservoirs of the nebulizer kit (*31*).

Bioaerosol Exposure of Microtubes

Nebulizers were secured to the two external threaded, brass ports of the exposure section with sterile 2.54 cm ID x 3.2 cm OD x 30 cm (L) clear PVC tubing (Fisher Scientific, Atlanta, GA). The bioaerosol chamber is raised on a platform so that the PVC tubing is situated as a straight horizontal path into the exposure section. This reduces the loss of bioaerosol on the sides of the PVC tubing before it reaches the exposure section. The nebulizers had all ports and openings closed in order to achieve the desired range of

bioaerosol size. The compressed air was delivered to the nebulizer at a speed of 8 L/min (*32*).

The exposure period was divided into a 30 min equilibration period and a 5 min static period. The equilibration period is the amount of time required to reach the desired bioaerosol concentration of 10^6 CFU/cm^3 within the exposure section. A volume of approximately 6 ml of the source concentration of 10^9 CFU/ml is required to bring the 6,125 cm^3 exposure section to an airborne concentration of 10^6 CFU/cm^3 in 30 min (*31, 32*).

The 5 min static period is initiated by discontinuing bioaerosol generation but not the imposed vacuum on the test cells. This period allows time for the bioaerosol to fall out as a result of gravitational sedimentation. It takes 5 min for the bacteria from the top of the exposure chamber to settle to the same level as the openings of the microtubes, which is approximately 6 cm.

The bioaerosol also, under these conditions, produces a relative humidity of 98% ± 1% (*31*).

Imposed pressure

Imposed pressures of 0, -6.89, -13.78, and –34.45 kPa (0, -1, -2, and –5 psi) were used as the pressure differential. Negative pressure was imposed on the internal vial of the test cell 5 min before the onset of the equilibration period by a compressor/vacuum pump model ROA-P131-AA (Gast, Benton Harbor, MI). General purpose rubber tubing with a 0.33 μm inline filter product no. 4210 (Gelman Sciences, Ann Arbor, MI), to filter air flowing into sterile test cells, was attached to the compressor and internal vial of test cell. A 500 ml side arm flask was used between the exposure chamber and the compressor to reduce pressure fluxuations to below 0.06 kPa (0.01 psi). An inline pressure gauge model HHP701-2 (Omega Engineering, Inc., Stamford, CT) with a detection range of 137.9 kPa positive and negative pressure, and a resolution of 0.05% and accuracy of ±0.15% FS, was used to measure the imposed pressure (*31*).

Detection of Positives

Test cells were aseptically removed from the exposure chamber. The tryptic soy broth was then aseptically transferred to a sterile vial, where the volume was brought up to 5 ml tryptic soy broth. Kanamycin (30 μg/ml) and tetracycline (10 μg/ml) were added to the 5 ml samples from fresh stocks of 5 mg/ml kanamycin and 1 mg/ml tetracycline. The vials were shaken at room temperature on an orbital shaker at 250 rpm for 72 hrs. A sample was determined to be positive if turbidity existed in the vial after 72 hrs of incubation.

Kanamycin and tetracycline resistance was confirmed by plating positive samples on tryptic soy agar containing kanamycin (30 μg/ml) and tetracycline (10 μg/ml).

Bioaerosol Concentration Confirmation

The bioaerosol concentration was measured during one run on each day. Two filter papers were cut into approximate sizes of 3 cm^2 and placed in the exposure section of the chamber at opposite ends on the panel where the microtubes were situated, in between the microtubes. After the bioaerosol test, the papers were aseptically removed from the chamber and transferred to separate flasks containing sterile Butterfield's phosphate buffer pH 6.8. The flasks were shaken at room temperature for 5 min. Then the buffer was serially diluted and plated on tryptic soy agar containing kanamycin (30 μg/ml) and tetracycline (10 μg/ml), (*31*).

Experimental Design

Since there are only three test chambers, and four imposed pressures to be tested, a randomized balanced incomplete block design was used for the bioaerosol challenge test. The blocks are the days that the chambers were run; the treatments are the imposed pressure and the microtube hydraulic diameters. The imposed pressure was randomized throughout the blocks to reduce block effects and the diameters were randomized within each experimental unit (test chamber) to reduce position effects. Each experimental unit received one of four imposed pressure treatments and all seven hydraulic diameter

treatments. There are three replicates of each experimental unit randomized throughout the incomplete block.

Data was analyzed by treating pressure and diameter as continuous variables in a logistic regression (*11*) using JMP® (SAS Institute, Cary, NC).

RESULTS AND DISCUSSION

Threshold Leak Size

Different food products were used to determine a range of surface tensions and densities to calculate threshold leak pressures. Package liquid fill heights were also quantified to the nearest centimeter for liquid static head calculations (ρ**gL**). The leak pressure was calculated as if the leak occurred at the bottom of the package, thus making **L** equal to the fill height in the container. The values obtained for liquid static heads were quite small. The largest container, the 5 liter wine box (approximately 20 cm fill height), only had a static head of 2 kPa. This affects the threshold pressure by only a small amount.

The major factors involved in the threshold leak pressure calculation are the surface tension, σ, and the microhole hydraulic diameter, $\mathbf{D_h}$. Microhole hydraulic diameters of 2, 5, 7, 10, 20, and 50 μm and length, **l**, of 7 mm were used to calculate leak pressures (*31*).

Using the threshold leak pressure equation {1}, the threshold pressures for various products were calculated for each microtube size (Table 3). Threshold leak size at a pressure greater than 6.9 kPa, (or less than –6.9 kPa) is approximately 7 μm for liquids of low surface tension (dyes, oil). The threshold leak size increases to 10 μm for mid-range surface tension products (dairy, beer, orange juice), then increases to a value between 10 μm and 20 μm for high surface tension products (juices, water).

Table 2 – Threshold pressures as calculated by equation {2}(*31*), in kPa, of products with surface tension, σ, at each microtube hydraulic diameter (50, 20, 10, 7, 5, and 2 μm).

			Threshold Pressures (kPa) at these hydraulic diameters					
LIQUID	**σ (mN/m)**	**ρgL(KPa)**	**50**	**20**	**10**	**7**	**5**	**2**
Alcohol								
dye, safranin red	21.40	0.06	0.64	1.65	3.32	4.75	6.65	16.67
dye, mineral spirits red	24.90	0.07	0.75	1.91	3.86	5.52	7.74	19.39
dye, Scarlett Moo	25.60	0.09	0.76	1.96	3.96	5.67	7.95	19.93
beer	47.35	1.49	0.90	3.11	6.81	9.97	14.19	36.35
wine, white zinfandel	50.72	1.88	0.85	3.22	7.18	10.57	15.09	38.83
vanilla extract	51.92	1.20	1.15	3.58	7.63	11.10	15.73	40.03
Oils								
oil, olive	33.12	1.13	0.59	2.14	4.73	6.94	9.89	25.39
oil, vegetable	33.25	1.43	0.48	2.04	4.63	6.85	9.82	25.38
Dairy								
milk, 2%	43.74	1.82	0.65	2.70	6.11	9.04	12.94	33.41
milk, half & half	43.81	0.98	0.98	3.03	6.45	9.38	13.29	33.79
milk, whole	43.89	1.82	0.66	2.71	6.14	9.07	12.98	33.52
milk, evaporated	48.87	1.13	1.08	3.37	7.18	10.45	14.81	37.68
milk, lactose free	49.17	1.82	0.82	3.13	6.96	10.25	14.63	37.64
milk, fat free	49.18	1.86	0.81	3.11	6.95	10.23	14.62	37.64
Aqueous								
dye, toluidine blue	30.70	0.10	0.92	2.36	4.75	6.80	9.54	23.91
juice, lemon	36.72	1.30	0.64	2.36	5.22	7.68	10.95	28.13
soup, chicken broth	43.55	1.06	0.95	2.98	6.38	9.29	13.17	33.56
coffee	44.10	1.90	0.63	2.70	6.14	9.09	13.02	33.66
juice, orange	47.30	1.91	0.73	2.94	6.63	9.80	14.01	36.15
soy sauce	47.59	1.92	0.74	2.96	6.68	9.86	14.10	36.37
tea, iced	55.72	1.57	1.13	3.73	8.08	11.81	16.77	42.85
juice, apple	58.28	1.85	1.10	3.82	8.37	12.27	17.46	44.74
juice fortified	63.90	2.12	1.17	4.16	9.14	13.41	19.11	49.02
juice, grape	68.41	2.02	1.35	4.55	9.88	14.46	20.56	52.57
deionized water	71.30	0.98	1.84	5.18	10.74	15.51	21.86	55.23

The calculated threshold leak pressures were compared to experimental imposed pressures required to form a droplet of radius R at the end of a microtube of the same radius, and hold the droplet at that size. The liquid samples used for these experimental numbers were deionized water, whole milk, soy sauce, and white Zinfandel wine. These samples were chosen because of their differences in composition. The soy sauce has a high concentration of soluble solids, the wine contains alcohol, whole milk contains proteins, micelles, and other small particulates that may clog a defect, and the deionized water is used as a control. All samples except the milk were filtered through Whatman No. 4 filters to eliminate large particulates. The imposed pressures measured for each of the samples were in the region of the calculated values except for the milk (Table 4). The milk sample did not even begin to leak through the 50 μm hole after 1 min of imposed pressure of 20.7 kPa. This is because there are proteins and other components in milk that obviously clog the defect. These measurements, along with the observations of Keller (*31*), confirm that the threshold leak pressure equation is a valid approximation tool only for filtered products.

Table 3 – Comparison of the experimentally observed values of the threshold leak pressures (kPa) and the values calculated using the threshold leak pressure equation {2} of soy sauce, wine, deionized water, and whole milk using microtubes with hydraulic diameters of 5, 10, and 50 μm. NR means no reading.

	Threshold Pressures (kPa) at Hydraulic Diameters 5, 10, and 50 μm		
LIQUID	**5**	**10**	**50**
Observed Values			
soy sauce	13.8	6.9	0.7
wine	15.2	3.5	0.7
deionized water	22.8	8.3	2.1
whole milk	NR	NR	>20.7
Calculated Values			
soy sauce	14.10	9.86	0.74
wine	15.09	7.18	1.15
deionized water	21.86	10.74	1.84
whole milk	12.98	6.14	0.66

Since the experimental hydraulic diameters are of known size, the surface tension becomes the main factor used to indicate leak initiation. The higher the surface tension value, the larger the imposed pressure must be at each hydraulic diameter to initiate liquid flow. Deionized water had the largest surface tension value of 71.3 mN/m and subsequently the largest imposed pressures at each hydraulic diameter required to initiate leaks. The lowest surface tensions measured were the dyes typically used in dye penetration testing: Methylene blue (30.7 mN/m), Scarlett Moo (25.6 mN/m), mineral spirits red (24.9 mN/m), and safranin red (21.4 mN/m). These dyes subsequently have the lowest threshold leak pressures associated with penetration into a microhole.

The largest difference between threshold pressures of products with low or high surface tensions occurs as microhole size decreases. Figure 1 graphically compares threshold pressure differences between the highest surface tension (deionized water), the lowest surface tension (safranin red dye), and two products that fall in between (2% milk and white Zinfandel wine). It can be seen on the graph that the difference between threshold pressures of deionized water and safranin red dye shows an increase as microhole size decreases.

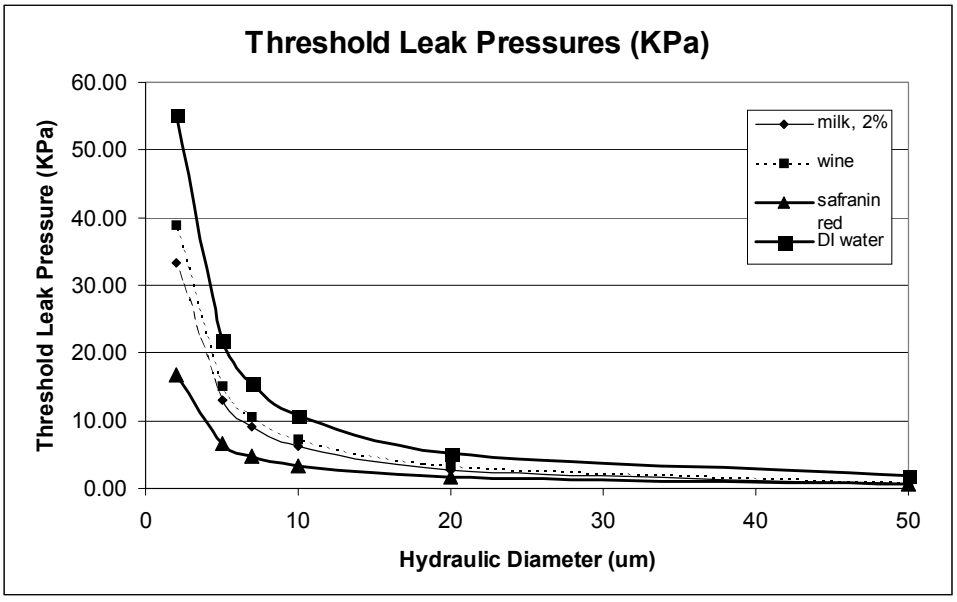

Figure 1– Graph of the threshold leak pressures at increasing hydraulic diameters of deionized (DI) water, white Zinfandel wine, 2% milk, and safranin red dye. The surface tension of these products is in order from highest (water) to lowest (dye).

Leak Rates

Once the threshold leak pressure is calculated, the Hagen-Poiselle equation {3} can be used to determine the volumetric rate of flow, **Q**. By definition, the pressure differential ($\mathbf{P_o}$-$\mathbf{P_L}$) is what drives the leak (*19, 43*). The term $\mathbf{P_L}$ is the threshold leak pressure. The imposed pressure $\mathbf{P_o}$ must be larger than $\mathbf{P_L}$ in order for the liquid of viscosity, **μ**, to leak out of the container through a defect with radius, **R**, and length, **l**. The radius is calculated as half of the hydraulic diameter: 1, 2.5, 3.5, 5, 10, and 25 μm. The length of the nickel microtubes is 7 mm. All pressure values were converted into pascals (1 psi = 6,895 Pa) before being entered into the Hagen-Poiselle volumetric flow rate equation.

Theoretical positive pressure differentials were inserted into the Hagen-Poiselle volumetric flow rate equation to examine probable leakage rates at increasing imposed pressures. For instance, deionized water with viscosity at 20°C being 0.001 Pa·s, leaking through a microhole with a hydraulic diameter of 10 μm and length of 7 mm, under a positive pressure differential of 34.5 kPa would have a volumetric flow rate of 0.105 cm^3/day (Fig. 2), whereas if the hydraulic diameter is increased to 20 μm, the leak rate leaps to 1.7 cm^3/day (Fig. 3).

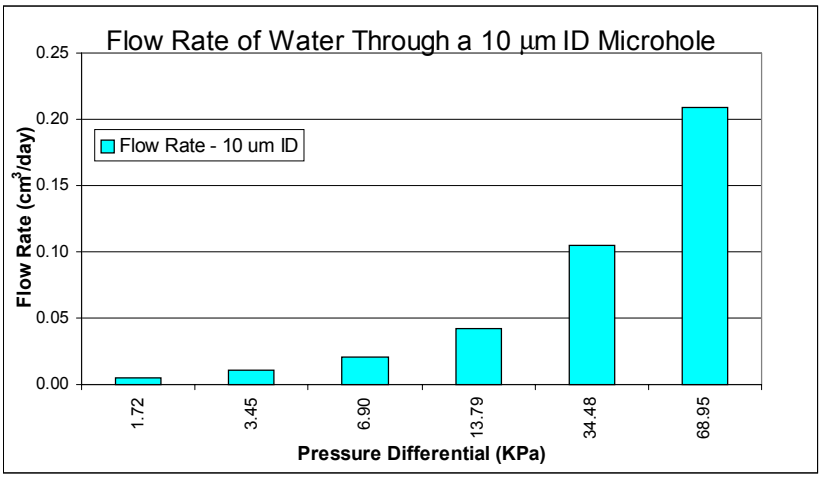

Figure 2 – Flow rate of deionized water through a 10 μm microhole.
As calculated from the Hagen-Poiselle flow rate equation {3}.

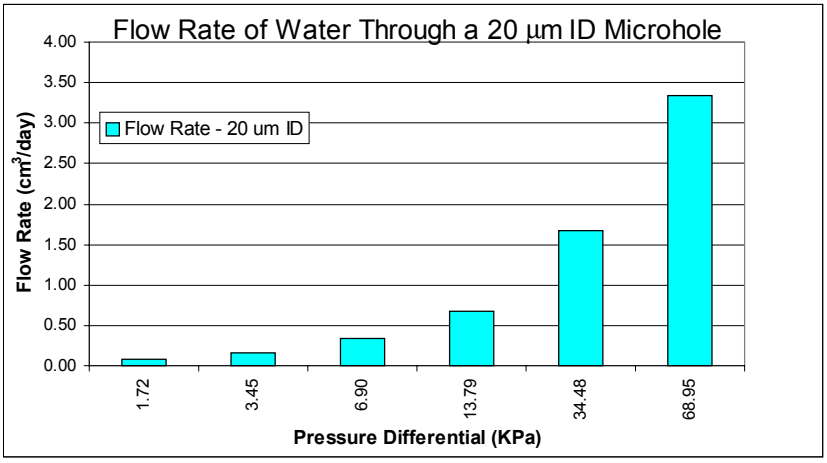

Figure 3 – Flow rate of deionized water through a 20 µm microhole.
As calculated from the Hagen-Poiselle flow rate equation {3}.

Evaporation Rate vs. Flow Rate

Since the leakage rates are so slow, it is thought that evaporation will play a major role in determining critical leakage. If the product leaks at such a slow rate that the evaporation rate exceeds the flow rate, then there will be no leak. It is believed that the water will evaporate leaving solids behind that will block the opening of the defect thus effectively resealing it (*15, 31*).

Evaporation rate is usually calculated as molar evaporation rate (gmol/s). Therefore, the volumetric flow rate must be converted to molar flow rate as described by equation {6} or the molar evaporation rate can be converted to a volumetric flow rate by multiplying the molar flow rate by the molecular weight, and then multiplying that result by the density of the liquid. For example, a droplet of water, having the same droplet radius as the 50 µm microhole, in an environment with 80% relative humidity, at room temperature, will evaporate at a molar rate of 6.17×10^{-9} gmol/s, or at a volumetric rate of 0.0096 cm^3/day. Increasing the droplet radius, or the surface area of the water exposed to the air will increase the evaporation rate.

Since food products contain soluble solids the question was raised about the effect of additives on the evaporation rate. The evaporation rate of a liquid with soluble solids may be calculated by substituting the vapor pressure of the liquid in question with the vapor pressure of water in equations 8 and 9. These vapor pressures can be found by

measuring the water activity, A_w, which is a ratio of the vapor pressure of a food product (P) to the vapor pressure of pure water (P_o) at the same temperature. Increasing the concentration of soluble solids in a liquid decreases the vapor pressure of that liquid. When the vapor pressure decreases from the vapor pressure of water, the water activity decreases and so does the evaporation rate. However, the evaporation rate does not drastically decrease as soluble solids content increases. The water activity was measured for soy sauce, 5 M NaCl, 2.5 M NaCl, and 1.25 M NaCl. Evaporation rates were calculated at 80% relative humidity for a droplet of the same radius as the opening it protrudes from.

Table 4 – Evaporation rates (cm^3/day) at 80% relative humidity, calculated for liquids with varying soluble solids content having droplet radius of 25 μm and water activity A_w.

		Evaporation Rate
LIQUID	**A_w**	**(cm^3/day)**
water	1.000	0.00959
soy sauce	0.830	0.00786
5 M NaCl	0.792	0.00765
2.5 M NaCl	0.899	0.00862
1.25 M NaCl	0.949	0.00913

Using deionized water as an example, it can be shown that the evaporation rate of water is greater than the flow rate of water through a microhole of 2 μm hydraulic diameter (Fig. 4). This is also the case through a 5 μm hydraulic diameter with a pressure differential of up to 6.9 kPa (Fig 5), and 7 μm and 10 μm hydraulic diameters with pressure differentials up to 3.45 kPa.

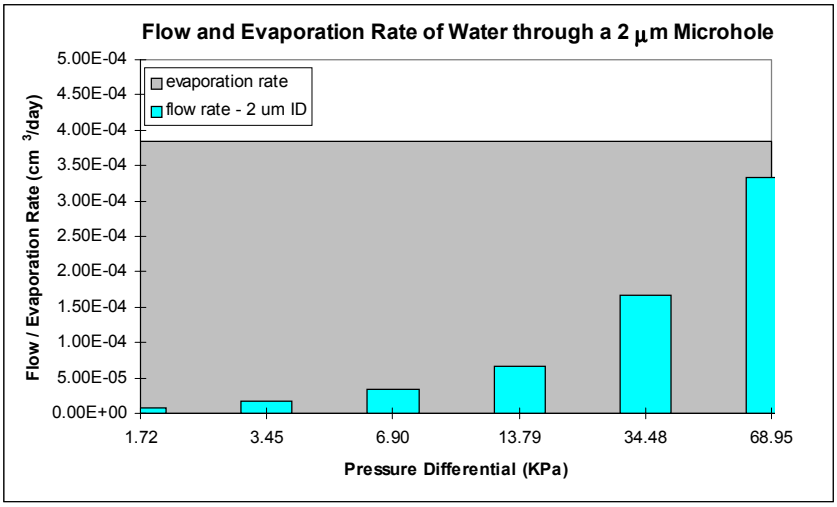

Figure 4 – Flow rate, calculated using equation {3}, and evaporation rate, calculated using equation {4}, of water through a 2 µm microhole under room temperature and 80% relative humidity. The shaded area represents evaporation. Any bar that lies totally within the shaded area means that the evaporation rate surpasses the flow rate. In this case, all flow rates are not fast enough to allow leakage to occur.

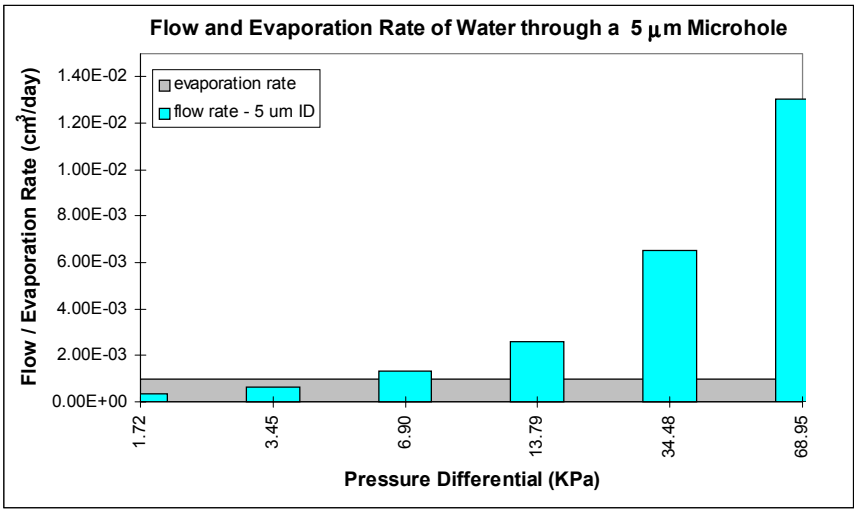

Figure 5 - Flow rate, calculated using equation {3}, and evaporation rate, calculated using equation {4}, of water through a 5 µm microhole under room temperature and 80% relative humidity. The shaded area represents evaporation. Any bar that lies totally within the shaded area means that the evaporation rate surpasses the flow rate. In this case, all flow rates are faster than the evaporation rate, except the 1.72 kPa and 3.45 kPa pressure differential driven leaks.

Microtube Size

The microtube diameters were measured using a microscope equipped with video calipers. Hydraulic diameters were calculated from these diameters using equation {2}.

Confirmation of Bioaerosol Concentration

Plate counts were made of the serial dilutions of the filter papers from the exposure section. They were within the range expected for an average bioaerosol concentration of 10^6 cfu/cm^3.

Critical Leak Size

The critical leak size was determined for air-filled defects to be approximately 7 μm for pressure differentials ranging from equilibrium (0 kPa) to -34.5 kPa. This includes the pressure differential of –6.9 kPa even though the smallest diameter that allowed microbial penetration for this particular pressure differential was 10 μm in this experiment.

The hydraulic diameter effects were significantly different ($p < 0.005$) while the pressure did not play a significant role in microbial ingress ($p > 0.05$). There was also no significant interaction between the pressure and hydraulic diameter ($p > 0.05$). This means that the difference between the microtube sizes was the only significant factor involved in the ingress of the indicator organism under these conditions.

When aerosol particles accumulate on the air-filled microtube and then start to enter the opening, the fluid flow dynamics become a liquid flow situation. Since the bacteria are aerosolized in Butterfield's phosphate buffer, which has a surface tension of 65 mN/m, threshold pressure must be reached in order for the buffer and bacteria to begin ingress into the microtube. Table 5 shows the threshold leak pressure of Butterfield's phosphate buffer for each diameter of microtube as well as the volumetric flow rates, Q.

Table 5 – Threshold leak pressure, P_L, of Butterfield's phosphate buffer for each hydraulic diameter of microtube calculated using equation {1}, and volumetric flow rate calculated using equation {3}, Q, of Butterfield's phosphate buffer. Units of cm^3/exposure is the volume leaking through the microtube during the 30 minute exposure.

Hydraulic Diameter (μm)	Threshold Leak Pressure P_L (kPa)	Volumetric Flow Rates Q (cm^3/s)	Q (cm^3/exposure)
50	1.59	3.43×10^{-5}	6.17×10^{-2}
20	4.62	2.58×10^{-6}	4.65×10^{-3}
10	9.65	3.39×10^{-7}	6.11×10^{-4}
7	14.00	1.18×10^{-7}	2.12×10^{-4}
5	19.79	1.11×10^{-9}	2.00×10^{-6}
2	50.26	2.82×10^{-9}	5.07×10^{-6}

Table 6 – Number of positives out of three replicates for microbial ingress at each imposed vacuum (0, -6.9, -13.8, -34.5 kPa) for each microtube hydraulic diameter (0, 2, 5, 7, 10, 20, and 50 μm).

Hydraulic Diameter (μm)	Imposed Vacuums 0 kPa	-6.9 kPa	-13.8 kPa	-34.5 kPa
0	0/3	0/3	0/3	0/3
2	0/3	0/3	0/3	0/3
5	0/3	0/3	0/3	0/3
7	1/3	0/3	2/3	3/3
10	1/3	1/3	2/3	1/3
20	3/3	0/3	3/3	2/3
50	3/3	3/3	3/3	3/3

The findings of the experiment coincide with Table 5 only partially. At an imposed pressure of 34.5 kPa, the threshold leak size appears to be 5 μm because it only requires 19.79 kPa of pressure to initiate the leak. While this may be the case using the threshold leak pressure equation {2}, other factors exist in this experimental set-up. The leak rate, for instance, may not be fast enough in the allotted time of the test run to allow the bacteria to traverse the microtube length. The leak rate at –34.5 kPa, through the 7

μm hole is 100 times faster than the leak rate of the 5 μm hole. This may be the reason that microbial penetration is seen at the 7 μm and not the 5 μm.

At the imposed pressure of -6.9 kPa, the critical leak size appears to be 10 μm from the experiment. The threshold leak pressure for the 10 μm hole is 9.65 kPa from Table 5. How can a leak occur if the threshold pressure has not been achieved? This question may be answered by simply stating that the threshold leak pressure equation is an approximation. The threshold may be breached by the capillary action of the buffer into the microtube or maybe the hole was large enough that the aerosol droplet did not completely cover the opening of the microtube, therefore rendering the threshold leak pressure equation inaccurate and non-predictive. Another explanation could be that surface oxidation of the nickel microtubes may reduce the imposed pressure required to initiate a leak (*31*).

This is also the case with the equilibrium, 0 kPa, pressure differential. From the threshold leak pressure equation, there should be no leaking of buffer or bacteria into the test cell. This, however, is not the observation from the experiment. The experimental data shows that the critical leak size is 7 μm at 0 kPa (Table 4).

The critical leak size should be a conservative number. This is why 7 μm was chosen as the critical leak size for all of the pressure differentials (Table 7). There is a degree of probability associated with the entry, and penetration of a bioaerosol particle through a microtube. This could explain the reason why one of the three replicates of the 0 kPa pressure differential was positive for microbial ingress at 7 μm and 10 μm, whereas none of the three replicates at –6.9 kPa pressure differential and 7 μm and 20 μm saw microbial penetration (Table 6).

To recap an earlier investigation (*24*), an immersion biotest was done using semi-rigid aseptic cup lids and retort trays with laser-drilled holes of diameters ranging from 10 - 20 μm. The holes in the aseptic cup lids were drilled from the outside to the inside, and the holes in the retort trays were drilled from the inside to the outside. The hole sizes were then measured on the inside and outside of the package after the biotest. For the aseptic cup lids, the hole on the outside was measured to be 10 μm before and after the test. The inside of the lid showed the hole to be 7 μm after the test (*24*). The retort trays

hole sizes could not be confirmed after the test so an estimation from the measurements of the aseptic cup lids hole sizes would be that the inside defect of the retort tray would be 10 µm and the outside defect would be approximately 7 µm. The data from the immersion test showed that the aseptic cup lids allowed microorganisms into the container at a higher percentage than the tests with the retort trays (*24*). Since the defects manufactured in the retort tray cannot be confirmed, a guess to their size would be less than 7 µm and quite possibly less than 5 µm. The threshold leak size has not been reached for the pressure that the liquid static head is exerting on the defect, so no liquid is entering the defect, thus there is no microbial ingress.

Table 7 – Critical Leak Size of an air-filled microtube at imposed pressures (0, -6.9, -13.8, and –34.5 kPa). An 'X' represents at least one positive out of 3 replicates. A '-' represents zero positives.

Hydraulic	IMPOSED PRESSURES			
Diameter (µm)	0 kPa	-6.9 kPa	-13.8 kPa	-34.5 kPa
0	-	-	-	-
2	-	-	-	-
5	-	-	-	-
7	X	-	X	X
10	X	X	X	X
20	X	-	X	X
50	X	X	X	X

Table 8 – Critical leak sizes at different imposed pressures for a liquid-filled microtube (*31*). The 'X' represents at least one positive out of 9 replicates and the '-' represents zero positives out of 9 replicates.

Hydraulic	IMPOSED PRESSURES						
Diameter (µm)	20.7 kPa	13.8 kPa	6.9 kPa	0 kPa	-6.9 kPa	-13.8 kPa	-20.7 kPa
0	-	-	-	-	-	-	-
2	-	-	-	-	-	-	-
5	X	X	-	-	-	X	X
7	X	X	-	-	-	X	-
10	X	X	-	-	-	X	X
20	X	X	X	-	-	X	X
50	X	X	X	X	X	X	X

Previous research has shown that the critical leak size of a liquid-filled defect, where the bacteria must penetrate upwards into the test cell against gravity, ranges from 5 to 20 μm (*31*). Table 8 shows that the critical leak size of positive and negative pressure with magnitudes of 13.8 and 20.7 kPa is 5 μm. When the pressure is reduced to between 6.9 and –6.9 kPa, the critical leak size drops to 20 and 50 μm (*31*). The reason that the critical leak size increases so much at the lower pressures is because the threshold leak size has not been reached, thus there is no liquid channel formed between the inside and the outside of the test cell. Since the test cells are upside-down, the bacteria require a medium by which to maneuver through the microtube and at the lower pressure differentials, that medium is not present.

CONCLUSIONS

The threshold leak pressures were calculated from density and surface tension measurements of a wide range of liquid food products and standard dyes used in dye penetration testing of package integrity. The threshold leak pressure equation can only be applied to liquid food products that have been filtered, as particulate matter in the liquid will clog even a 50 μm defect. Considering typical pressures generated within a food package ($P_o \leq \pm 34.5$ kPa), a defect with a 2 μm hydraulic diameter will never reach the threshold pressure for most filtered liquid food products.

Even if the threshold pressure were breached, the leak rate would be slower than the evaporation rate, resulting in no net leakage. Also, since most filtered liquid food products are not pure water, if the evaporation rate is faster than the leak rate, then soluble solids may also be left behind, thus effectively resealing the leak.

The critical leak size of an air-filled defect was experimentally determined, by bioaerosol exposure, to be approximately 7 μm for pressure differentials ranging from equilibrium (0 kPa) to -34.5 kPa. This is slightly different than the previous results of a liquid-filled defect, in which the critical leak size coincided with the threshold leak size.

REFERENCES

1. Amini, M. A., and D. R. Morrow. 1979. Leakage and permeation: theory and practical applications. Package Dev. and Sys. May/June: 20-27.

2. Anderson, G. L. 1989. Leak testing. p.50-57. *In* 9th ed. Nondestructive evaluation and quality control: metals handbook. AOAC International, Rockville, MD.

3. Anema, P. J., and B. L. Schram. 1980. Prevention of post-process contamination of semi-rigid and flexible containers. J. Food Prot. 43(6):461-464.

4. Bankes, P., and M. F. Stringer. 1988. The design and application of a model system to investigate physical factors affecting container leakage. Int. J. Food Micro. 6:281-286.

5. Bausum, H. T., S. A. Schaub, K. F. Kenyon, and M. J. Small. 1982. Comparison of coliphage and bacterial aerosols at a wastewater spray irrigation site. Appl. Environ. Microbiol. 43(1):28-38.

6. Blakistone, B. A. 1996. EU/USA status report: the current issues in plastic packaging seal evaluation in Europe and the USA. Pack. Technol. 13(3):

7. Blakistone, B. A., S. W. Keller, J. E. Marcy, G. H. Lacy, C. R. Hackney, and W. H. Carter, Jr. 1996. Contamination of flexible pouches challenged by immersion biotesting. J. Food Prot. 59(7):764-767.

8. Bovallius, A., B. Bucht, R. Roffey, and P. Anas. 1978. Long-range air transmission of bacteria. Appl. Environ. Microbiol. 35(6):1231-1232.

9. Bryant, M. 1988. Packaging failures: quality in design doesn't end with the finished product. Med. Dev. & Diag. Ind. 10(8):30-33.

10. Butler, L. D., J. J. Coupal, and P. P. DeLuca. 1978. The detection of ampul leakers using short-lived radionuclides. J. Parenter. Drug Assoc. 32(1): 2-9.

11. Carter, H. W. 2000. Personal Communication. Chair of Biostatistics Department, Medical College of Virginia, Richmond, VA.

12. Chen, C., B. Harte, C. Lai, J. Pestka, and D. Henyon. 1991. Assessment of package integrity using a spray cabinet technique. J. Food Prot. 54(8):643-647.

13. Clark, S. R. Rylander, and L. Larsson. 1983. Airborne bacteria, endotoxin and fungi in dust in poutry and swine confinement buildings. Am. Ind. Hyg. Assoc. J. 44(7):537-541.

14. Davidson, P. M., and I. J. Pflug. 1981. Leakage potential of swelled cans of low-acid foods collected from supermarkets. J. Food. Prot. 44(9):692-695.

15. Davis, R. M. 1999. Personal Communication. Associate Professor, Chemical Engineering, Virginia Polytechnic Institute and State University, Blacksburg, VA.

16. Dimmick, R. L., H. Wolochow, and M. A. Chatigny. 1979. Evidence for more than one division of bacteria within airborne particles. Appl. Environ. Microbiol. 38(4):642-643.

17. Gilchrist, J. E., U. S. Rhea, R. W. Dickerson, and J. E. Campbell. 1985. Helium leak test for micron-sized holes in canned foods. J. Food Prot. 48(10):856-860.

18. Gilchrist, J. E., D. B. Shah, D. C. Radle, and R. W. Dickerson, Jr. 1989. Leak detection in flexible retort pouches. J. Food Prot. 52(6):412-415.

19. Guazzo, D.M. 1994. Package Integrity Testing, p. 247-276. *In* M. J. Akers (ed.), Parenteral quality control: sterility, pyrogen, particulate, and package integrity testing, 2nd ed Mercel Dekker, New York.

20. Hackett, E. T. 1996. Dye penetration effective for detecting package seal defects. Packag. Tech. Eng. 8:49-52.

21. Harper, C. L., B. A. Blakistone, J. B. Litchfield, S. A. Morris. 1995. Developments in food packaging integrity testing. Trends in Food Sci. and Technol. 6(10):336-340.

22. Hoffman, W. 1996. Cooperative research and development agreement. Philips Laboratory, OLAC PL/RKFE. Edwards, CA.

23. Howard, G., and R. Duberstein. 1980. A case of penetration of 0.2 mm rated membrane filters by bacteria. J. Parenter. Drug Assoc. 34(2):95-102.

24. Hurme, E. U., G. Wirtanen, L. Axelson-Larsson, N. A. M. Pachero, and R. Ahvenainen. 1997. Penetration of bacteria through microholes in semirigid aseptic and retort packages. J. Food Prot. 60(5):520-524.

25. Hurme, E. U., and R. Ahvenainen. 1998. A nondestructive leak detection method for flexible food packages using hydrogen as a tracer gas. J. Food Prot. 61(9):1165-1169.

26. Jackson, G (ed.). 1995. Bacteriological Analytical Manual, 8th ed. p.3.64. Food and Drug Administration. AOAC International, Rockville, MD.

27. Jarrosson, B. P. 1992. Closure integrity testing of heat sealed aseptic packaging using scanning acoustic microscopy. M.S. Thesis, Virginia Polytechnic Institute and State University, Blacksburg, VA.

28. Kamei, T., J. Sato, A. Natsume, and K. Noda. 1991. Microbiological quality of aseptic packaging and the effect of pinholes on sterility of aseptic products. Pack. Technol. and Sci. 4:185-193.

29. Keller, S., J. E. Marcy, B. A. Blakistone, and G. H. Lacy. 1995. Package integrity biotesting: aerosol versus immersion. *In* T. Ohlsson (ed.). Proceedings of the International Symposium Advances in Aseptic Processing and Packaging Technologies. SIK, Goteborg, Sweden.

30. Keller, S., J. E. Marcy, B. A. Blakistone, G. H. Lacy, C. R. Hackney, and W. H. Carter, Jr. 1996. Bioaerosol exposure method for package integrity testing. J. Food Prot. 59(7):768-771.

31. Keller, S. 1998. Determination of the leak size critical to package sterility maintenance. Ph.D. Dissertation, Virginia Polytechnic Institute and State University, Blacksburg, VA.

32. Keller, S. Personal communication.

33. Kelsey, R. J. 1990. The status of leak detection. Food and Drug Pack. 11:8-21.

34. Lacy, G. H. 1999. Personal communication. Professor, Plant Pathology, Physiology and Weed Science, Virginia Polytechnic Institute and State University, Blacksburg, VA.

35. Lake, D. E., R. R. Graves, R. S. Lesniewski, and J. E. Anderson. 1985. Post-processing spoilage of low-acid canned foods by mesophilic anaerobic sporeformers. J. Food Prot. 48(3):221-226.

36. Lampi, R. A. 1980. Retort pouch: the development of a basic packaging concept in today's high technology era. J. Food Process Eng. 4:1-18.

37. Lenhart, S. W., S. A. Olenchock, and E. C. Cole. 1982. Viable sampling for airborne bacteria in a poultry processing plant. J. Toxicol. Environ. Health. 10:613-619.

38. McEldowney, S., and M. Fletcher. 1988. Bacterial desorption from food container and food processing surfaces. Microb. Ecol. 15:229-237.

39. McEldowney, S., and M. Fletcher. 1990a. A model system for the study of food container leakage. J. Appl. Bacteriol. 69:206-210.

40. McEldowney, S., and M. Fletcher. 1990b. The effect of physical and microbiological factors on food container leakage. J. Appl. Bacteriol. 69:190-205.

41. Michels, M. J. M., and B. L. Schram. 1979. Effect of handling procedures on the post-process contamination of retort pouches. J. Appl. Bacteriol. 47:105-111.

42. Morris, S. A., A. Ozguler, and W. D. O'Brien, Jr. May 21, 1999. "New sensors help improve heat-seal microleak detection." (Packaging Technology and Engineering Feature). [Internet, WWW]. ADDRESS: http://www.napco.com/pte/0798sensors.html.

43. Morton, D. K. 1987. Container/closure integrity of parenteral vials. J. Parenter. Sci. Technol. 41(5):145-158.

44. Morton, D. K., N. G. Lordi, L. H. Troutman, and T. J. Ambrosio. 1989. Quantitative and mechanistic measurements of container/closure integrity: bubble, liquid, and microbial leakage tests. J. Parenter. Sci. Technol. 43:104-108.

45. Pflug, I. J., P. M. Davidson, and R. G. Holcomd. 1981. Incidence of canned food spoilage at the retail level. J. Food Prot. 44(9):682-685.

46. Placencia, A. M., G. S. Oxborrow, and J. T. Peeler. 1986. Package integrity methodology for testing the biobarrier of porous packaging. part II: FDA exposure-chamber method. Med. Dev. & Diag. Ind. 8(4)46-53.

47. Put, H. M. C., H. T. Witvoet, and W. R. Warner. 1972. Mechanism of microbiological leaker spoilage of canned foods: a review. J. Appl. Bacteriol. 35:7-27.

48. Put, H. M. C., H. T. Witvoet, and W. R. Warner. 1980. Mechanism of microbiological leaker spoilage of canned foods: biophysical aspects. J. Food Prot. 43(6):488-497.

49. Raabe, O. G. (ed.). 1976. The generation of aerosols of fine particles. p.57-68. *In* Fine particles, aerosol generation, measurement, sampling, and analysis. Academic Press, Inc. New York, NY.

50. Reich, R. R. 1985. A method for evaluating the microbial barrier properties of intact packages. Med. Dev. and Diag. Ind. 7(3):80-88.

51. Sheehan, M. J., and J. V. Giranda. 1994. Bioaerosol generation in a food processing plant: a comparison of production and sanitation operations. Appl. Occup. Environ. Hyg. 9(5):346-352.

52. Spitzley, J. 1993. How effective is microbial challenge testing for intact sterile packaging? Med. Dev. and Diag. Ind. 15(8):44-46.

53. Stauffer, T. 1990. Non-destructive testing on flexible packaging. J. Pack. Technol. July/August:27-29.

54. Stauffer, T. 1995. On and off line leak detection of containers and packages. *In* Activities report of the R & D associates. 47(1):8-18. Research and Development Associates for Military Food and Packaging Systems, Inc. New York, NY.

55. Stersky, A., E. Todd, and H. Pivnick. 1980. Food poisoning associated with post process leakage (PPL) in canned foods. J. Food. Prot. 43(6):465-476.

56. Teltsch, B., H. I. Shuval, and J. Tadmor. 1980. Die-away knetics of aerosolized bacteria from sprinkler application of wastewater. Appl. Environ. Microbiol. 39(6):1191-1197.

57. Thompson, P. J., and M. A. Griffith. 1983. Identity of mesophilic anaerobic sporeformers cultured from recycled cannery cooling water. J. Food Prot. 46(5):400-402.

Vita

The author, Matthew Joseph Gibney IV, was born in Biloxi, Mississippi on February 27, 1973. He is the first son out of six children born to Dr. Sheila A. Gibney and Dr. Matthew J. Gibney III who reside in McLean, Virginia. Matt graduated in 1991 from the Thomas Jefferson High School for Science and Technology. He matriculated to Virginia Polytechnic Institute and State University where he studied microbiology and immunology and earned a B. S. degree in 1995.

During the spring semester of 1995, Matt began work at a biotechnology company, CropTech, in Blacksburg, Virginia. For the next four years he learned much about the biotechnological techniques required for creating transgenic tobacco plants and the recovery of the transgenic protein.

After learning of the lucrative careers in the food industry, Matt enrolled in the Food Science and Technology M. S. degree program at Virginia Tech in 1999. It was in this program where he became interested in the packaging aspects of food and pharmaceutical production.